

# Extended Scalar Particle Solutions in Black String Spacetimes with Anisotropic Quintessence

M.L. Deglmann <sup>a</sup>, B.V. Simão <sup>a</sup>, C.C. Barros Jr. <sup>a</sup>

<sup>a</sup>*Departamento de Física, Universidade Federal de Santa Catarina (UFSC), Campus Universitário Trindade, Florianópolis, 88035-972, Santa Catarina, Brazil*

---

## Abstract

We present new solutions to the Klein-Gordon equation for a scalar particle in a black string spacetime immersed in an anisotropic quintessence fluid surrounded by a cloud of strings, extending the analysis presented in our previous work. These novel solutions are dependent on the quintessence state parameter,  $\alpha_q$ , and are now valid for a much larger domain of the radial coordinate. We investigate the cases when  $\alpha_q = 0, 1/2, 1$ , encompassing both black hole and horizonless scenarios. We express the resulting radial wave functions using the confluent and biconfluent Heun functions, with special cases represented by Bessel functions. We derive restrictions on the allowed quantum energy levels by imposing constraints on the Heun parameters to ensure polynomial solutions. Furthermore, we investigate the emergence of "dark phases" associated with the radial wave function, focusing on the interesting case of  $\alpha_q = 1$ . Our findings provide insights into the dynamics of scalar particles in this complex spacetime and the potential impact of dark energy on quantum systems.

*Keywords:* Dark energy, Quintessence, Black strings, Spin-0 particle, Heun functions

---

## 1. Introduction

Over the past decades, several independent observations have provided strong evidence for the accelerated expansion of the Universe. Astrophysical

---

*Email addresses:* [m.l.deglmann@posgrad.ufsc.br](mailto:m.l.deglmann@posgrad.ufsc.br) (M.L. Deglmann ) ,  
[vallin.brana@posgrad.ufsc.br](mailto:vallin.brana@posgrad.ufsc.br) (B.V. Simão ) , [barros.celso@ufsc.br](mailto:barros.celso@ufsc.br) (C.C. Barros Jr. )

data derived from the luminosity distances of Type Ia supernovae [1, 2], along with data from the cosmic microwave background (CMB), baryon acoustic oscillations (BAO), and large-scale structure (LSS), consistently point to the existence of an unknown dark component, referred to as dark energy (DE), driving this expansion (see, for instance, [3, 4, 5]).

Different hypotheses for dark energy have been proposed [3], including the cosmological constant, which has long been the preferred candidate in the  $\Lambda$ CDM model of cosmology. However, due to some specific challenges and limitations of  $\Lambda$ , such as the fine-tuning and coincidence problems [3], active research has focused on alternative dark energy candidates. One of the most interesting ones is the quintessence model, created by Caldwell, Dave, and Steinhardt [6].

Five years after Caldwell et al.'s work [6], Kiselev [7] proposed an energy-momentum tensor for an anisotropic fluid with negative pressures along the radial ( $\rho$ ), azimuthal ( $\varphi$ ), and axial ( $z$ ) directions. This fluid, also termed quintessence, is distinct from models directly associated with a scalar field. Kiselev's original quintessence describes a time-independent fluid surrounding a black hole (BH), offering a simpler way to investigate dark energy and its physical consequences. Numerous studies have explored this approach, many of them incorporating a cloud of strings (CS) [8] alongside the quintessential fluid in the spacetime background (see, for example, [9, 10, 11, 12, 13, 14, 15, 16, 17, 18, 19, 20]).

Recent findings from the Dark Energy Spectroscopic Instrument (DESI) suggest that observational data favor a dynamical dark energy model [21, 22, 23, 24], implying time-varying models like the quintessence from Caldwell, Dave, and Steinhardt are favored. Further insights into the dark energy equation of state and its constraints can be found in [25, 26].

However, when considering a specific cosmic epoch where time-dependence may be negligible, it remains valuable to investigate the physical implications of a given dark energy scenario on both the structure of spacetime and the matter content within this background. Understanding the effects, particularly quantum effects, originating from this quintessential fluid is necessary. Comparing different scenarios (with or without CSs and/or BHs) in various spacetime geometries is crucial for a complete understanding, allowing us to link the results.

To explore the quantum effects due to quintessence, we may start the investigation with spin-0 particles governed by the Klein-Gordon (KG) equation, which is simpler than the Dirac equation yet equally important. The

investigation of spin-0 particles is a convenient way to explore a variety of physical systems, regardless of the context [27, 28, 29, 30, 31, 32, 33, 34, 35].

Motivated by the preceding discussion, our previous work [36] involved the analysis of an anti-de Sitter (AdS) spacetime. This spacetime comprised a black string (BS) [37, 38], a Kiselev quintessence fluid, and an analogue of clouds of strings, extending the configuration studied by Ali et al. [39]. The choice for this model has been motivated by the fact that it is built in terms of these fundamental elements, with the purpose of studying the effect of each one of them on the behavior of quantum systems inside this background. We focused on identifying admissible ranges for the parameters defining the spacetime geometry – namely, the cloud of strings parameter ( $\bar{a}$ ), the Schwarzschild-like radius ( $\rho_s$ ), and the quintessence parameter ( $N_q$ ) – and examining their influence on the metric function  $A(\rho)$ .

We also investigated the solution of the Klein-Gordon equation for a spin-0 particle near the event horizon, providing details for possible scenarios in this regime. To do so, we have used the confluent Heun equation [40]. In general, Heun equations are an excellent tool to handle exact solutions of physical systems. See, for example, the works of [41, 42, 43, 44, 45, 46].

For the specific case when the quintessence state parameter  $\alpha_q$  equals  $1/2$ , we had defined a quantum observable termed the “dark phase”, associated with the radial wave function of the particle. In principle, this dark phase could be determined for other values of  $\alpha_q$ , offering a new perspective on the effects of a dark energy candidate on quantum systems. Following our work, this system was also investigated by Ahmed and collaborators [47].

In the present work, we aim to extend our previous analysis by deriving new solutions to the Klein-Gordon equation that are valid over a much larger domain of the radial coordinate. These original solutions provide insights into particle dynamics in various scenarios, including black strings and horizonless cases. We investigate the cases where the quintessence state parameter,  $\alpha_q$ , takes the values  $0$ ,  $1/2$ , and  $1$ . This allows us to express the radial wave function using the confluent and biconfluent Heun functions, with special cases represented by Bessel functions. Furthermore, we delve into the constraints imposed on quantum energy levels, including those relevant to horizonless scenarios.

Finally, we investigate the emergence of dark phases within the scope of these extended solutions. Although our analysis is conducted in a cylindrically symmetric spacetime, we still pay particular attention to the limiting case of  $\alpha_q = 1$  (which corresponds to  $\omega_q = -1$ ). This specific case is of

significant interest as cosmological observations [3, 48, 24] suggest that the state parameter of present-day dark energy in our Universe is very close to this value.

This work is organized as follows: Section 2 provides a summary of the key findings from [36], including the metric, parameter estimates, the radial Klein-Gordon equation within this spacetime, and the solution for a scalar particle near the event horizon. In sections 3–5, we investigate the radial wave function for the cases where  $\alpha_q = 0, 1/2, 1$ , respectively, across a broader domain of the radial coordinate. Section 6 examines the emergence of dark phases within the context of these extended solutions, and finally, section 7 presents our concluding remarks. Appendix A presents the Confluent Heun equation and its local solutions using the Frobenius method. Appendix B examines the biconfluent Heun equation and its corresponding series solution.

## 2. Preliminary results

This section summarizes the findings of our prior work [36]. We review the cylindrically symmetric AdS spacetime incorporating a black string, anisotropic quintessence, and a cloud of strings. We then revisit event horizon formation criteria and admissible parameter ranges. Next, we present the results for the radial Klein-Gordon equation, including the effective potential  $V_{\text{eff}}(\rho)$ , which is crucial for our subsequent analysis. Finally, we revisit our initial solution near the event horizon to evaluate its strengths and limitations.

Let us start by considering the interval

$$ds^2 = A(\rho) c^2 dt^2 - \frac{d\rho^2}{A(\rho)} - \rho^2 d\varphi^2 - \frac{\rho^2}{l^2} dz^2, \quad (1)$$

associated with the ansatz of a black string [39]. Note that  $A(\rho) \in \mathbb{R}$ , the cylindrical coordinates are the standard  $\rho$ ,  $\varphi$ , and  $z$ , and that we have chosen to work in the convention of SI units. In addition,  $l$  is the AdS radius, satisfying  $l^2 = -3/\Lambda$ , with  $\Lambda$  being the cosmological constant. The components of the Einstein tensor for this metric take the form of

$$G_t^t = G_\rho^\rho = \frac{1}{\rho} \frac{dA}{d\rho} + \frac{A}{\rho^2}, \quad (2)$$

$$G_\varphi^\varphi = G_z^z = \frac{1}{2} \frac{d^2 A}{d\rho^2} + \frac{1}{\rho} \frac{dA}{d\rho}. \quad (3)$$

Taking the symmetry of the Einstein tensor into account, we introduce two matter components: the quintessence anisotropic fluid and a matter contribution similar to a cloud of strings [8], both satisfying the conservation of energy-momentum. Similar to [39], we describe the quintessence fluid according to

$$\begin{aligned} T_t^t &= T_\rho^\rho = \rho_q(\rho), \\ T_\varphi^\varphi &= T_z^z = \alpha_q \rho_q(\rho), \end{aligned} \quad (4)$$

where

$$\alpha_q = -\frac{1}{2}(3\omega_q + 1), \quad (5)$$

with  $-1 < \omega_q < -1/3$ . The state parameter  $\alpha_q$  is constant (time-independent) and takes values in the interval  $0 < \alpha_q < 1$ . The non-trivial components of this quintessential fluid are its energy density  $\rho_q$  and its radial and tangent pressures, identified as  $p_\rho = -T_\rho^\rho$ ,  $p_\varphi = -T_\varphi^\varphi$  and  $p_z = -T_z^z$ , in accordance with our *mostly-minus* sign convention for the metric tensor. In general the fluid is anisotropic, unless  $\alpha_q = 1$  occurs (in the limiting case of  $\omega_q = -1$ ).

Our additional matter component is analogous to the so-called “clouds of strings” [8] and is described by:

$$\begin{aligned} T_t^t &= T_\rho^\rho = \frac{a}{\rho^2}, \\ T_\varphi^\varphi &= T_z^z = 0, \end{aligned} \quad (6)$$

where  $a$  is a positive real constant.

We solved the Einstein equations

$$G_\mu^\nu + \Lambda \delta_\mu^\nu = \frac{8\pi G}{c^4} T_\mu^\nu \quad (7)$$

by combining the components of the Einstein tensor (2) and (3) with the energy-momentum tensor from quintessence (4), together with the one from clouds of strings, given by (6). Under these considerations, the solution for  $A(\rho)$  reads

$$A(\rho) = \bar{a} + \frac{\rho^2}{l^2} - \frac{\rho_s}{\rho} + N_q \rho^{2\alpha_q}, \quad (8)$$

where the cloud parameter  $\bar{a} = (8\pi G/c^4) a$ , the Schwarzschild-like radius  $\rho_s$ , and the quintessence parameter  $N_q$  are all positive real constants. In terms of SI units,  $\bar{a}$  is dimensionless,  $\rho_s$  has units of length (in m), while  $N_q$  has units

of  $m^{-2\alpha_q}$ . We estimated typical values for  $\bar{a}$  to be in the range  $10^{-6} - 10^1$  [36], while  $\rho_s$  would probably range from  $10^{-2}$  m to  $10^{15}$  m. Regarding  $N_q$ , we showed that it would depend on the amount of dark energy in the universe (with observable radius  $\rho_{obs.}$ ), and on the state parameter  $\alpha_q$ . In fact, we expect  $N_q$  to decrease exponentially with the increase in  $\alpha_q$ . That behavior would imply the estimated values of  $N_q$  to be those of table 1 for a large universe with  $\rho_{obs.} = 3.8 \times 10^{26}$  m. At last, the quintessence energy density is

$\omega_q$	$\alpha_q$	Estimate for $N_q$
-1/3	0	8.9 m <sup>0</sup>
-2/3	1/2	10 <sup>-26</sup> m <sup>-1</sup>
-1	1	10 <sup>-52</sup> m <sup>-2</sup>

Table 1: Estimates for  $N_q$  considering  $\rho_{obs.} = |l| = 3.8 \times 10^{26}$  m, with the amount of dark energy in the observable universe,  $E_{DE}$ , being of the order  $2 \times 10^{71}$  kg m<sup>2</sup> s<sup>-2</sup>.

given by

$$\rho_q = (2\alpha_q + 1) \frac{N_q}{8\pi G/c^4} \rho^{2\alpha_q - 2}.$$

It is relevant to note that, when  $\alpha_q = 0$ , the quintessence fluid behaves exactly as the string clouds (6) and this will be evident in our solutions of section 3. The radial pressure  $p_\rho$  is simply  $p_\rho = -\rho_q$ , as determined by eq. (4). Similarly, the radial dependence for the tangent and longitudinal pressures,  $p_\varphi$  and  $p_z$ , also follow from eq. (4) and are given by  $p_\varphi = p_z = -\alpha_q \rho_q(\rho)$ , with  $\rho_q$  given above. Notably, they are indeed negative pressures.

### 2.1. Event horizon

The system consisting of a black string, quintessence fluid, and a cloud of strings admits a nontrivial event horizon  $\rho_+$  if  $\rho_s \neq 0$ , unless we set  $\Lambda = \bar{a} = N_q = 0$ . We present cases of  $\rho_+$  depending on  $\alpha_q$  and its respective constraints in table 2. Note that  $N_{ql}$  in the third row is the sum of  $N_q$  with  $1/l^2$ .

In the case of *cloudless* scenarios, i.e.,  $\bar{a} = 0$ , the situation is simpler, and it is summarized in table 3. Our final scenarios are: absence of quintessence (with  $\bar{a} \neq 0$ ,  $\rho_s \neq 0$ ) together with the case where we remove the quintessential fluid as well as the clouds of strings, i.e.,  $\bar{a} = 0$  and  $N_q = 0$ . However, one should note that these last scenarios are special cases of table 2 (first row) and of table 3 (third row), just setting  $N_q = 0$ .

$\alpha_q$	$\rho_+$	Constraints
0	$\rho_s/(\bar{a} + N_q)$	$\rho_+^2/l^2 \ll 1$
1/2	$\rho_s/\bar{a}$	$\rho_+^2/l^2 \ll 1$ and $N_q \rho_s/\bar{a}^2 \ll 1$
1	$\rho_s/\bar{a}$	$N_{ql} \rho_s^2/\bar{a}^3 \ll 1$

Table 2: Results of  $\rho_+$  according to values of the state parameter  $\alpha_q$ .

$\alpha_q$	$\rho_+$	Constraints
0	$\rho_s/N_q$	$\rho_+^2/l^2 \ll 1$
1/2	$(\rho_s/N_q)^{1/2}$	$\rho_+^2/l^2 \ll 1$
1	$(\rho_s/N_{ql})^{1/3}$	None

Table 3: Determination of  $\rho_+$  according to values of the state parameter  $\alpha_q$  in the cloudless scenario.

## 2.2. The Klein-Gordon equation

In this work, we study scalar bosons within the spacetime defined by eq. (1). The behavior of these particles can be described by the Klein-Gordon equation in this metric. The general form of the Klein-Gordon equation is:

$$\frac{1}{\sqrt{-g}} \partial_\mu \left( g^{\mu\nu} \sqrt{-g} \partial_\nu \phi \right) + \frac{m_\phi^2 c^2}{\hbar^2} \phi = 0,$$

where  $g = \det(g_{\mu\nu})$ , and  $m_\phi$  represents the mass of the spin-0 particle. To solve this equation, we employ a separation of variables to show that the problem reduces to

$$\phi = e^{-iEt/\hbar} e^{in_R \varphi} e^{izk_z/l} R(\rho), \quad (9)$$

where  $E$  is the particle's energy,  $n_R \in \mathbb{Z}$ , while  $k_z \in \mathbb{R}$  is related to the particle's momentum along the  $z$ -axis. The radial equation for  $R(\rho)$  is given by

$$\partial_\rho^2 R(\rho) + \chi(\rho) \partial_\rho R(\rho) + \tau(\rho) R(\rho) = 0, \quad (10)$$

with

$$\chi(\rho) := \frac{1}{A(\rho)} \partial_\rho A + \frac{2}{\rho},$$

$$\tau(\rho) := \frac{1}{A(\rho)} \left( \frac{\epsilon^2}{A(\rho)} - \frac{\kappa^2}{\rho^2} - \bar{m}_\phi^2 \right).$$

The parameters  $\epsilon$ ,  $\kappa$ , and  $\bar{m}_\phi$  occurring in  $\tau(\rho)$  are defined by

$$\epsilon = \frac{E}{\hbar c}, \quad (11a)$$

$$\kappa^2 = n_R^2 + k_z^2, \quad (11b)$$

$$\bar{m}_\phi = \frac{m_\phi c}{\hbar}. \quad (11c)$$

When written in the Liouville normal form (A.11), the problem of solving eq. (10) becomes the one of determining

$$R(\rho) = \frac{R_0}{\rho \sqrt{A(\rho)}} u(\rho), \quad (12)$$

where  $R_0$  is a normalization constant, while the auxiliary function  $u(\rho)$  satisfies

$$u''(\rho) + V_{\text{eff}}(\rho) u(\rho) = 0. \quad (13)$$

The effective potential  $V_{\text{eff}}(\rho)$  is determined by

$$V_{\text{eff}}(\rho) = \frac{A'(\rho)^2 + 4\epsilon^2}{4A(\rho)^2} - \frac{1}{A(\rho)} \left[ \frac{1}{2} A''(\rho) + \frac{A'(\rho)}{\rho} + \frac{\kappa^2}{\rho^2} + \bar{m}_\phi^2 \right], \quad (14)$$

where  $\epsilon$ ,  $\kappa$ , and  $\bar{m}_\phi$  were conveniently defined by eqs. (11a)–(11c).

When we assume the existence of a nontrivial event horizon  $\rho_+$ , it is convenient to define a new dimensionless coordinate  $x$ , so that

$$x = \frac{\rho}{\rho_+}, \quad (15)$$

with  $x \in (0, +\infty)$ . In fact, when looking for solutions where  $\rho_s \neq 0$ , we solve the problem for  $x > 1$ , i.e., outside the event horizon (to describe observable particles). In terms of the new variable  $x$ , eqs. (13) and (14) become

$$u''(x) + \rho_+^2 V_{\text{eff}}(x) u(x) = 0, \quad (16)$$

with

$$\rho_+^2 V_{\text{eff}}(x) = \frac{A'(x)^2 + 4(\rho_+ \epsilon)^2}{4A(x)^2} - \frac{1}{A(x)} \left[ \frac{1}{2} A''(x) + \frac{A'(x)}{x} + \frac{\kappa^2}{x^2} + \rho_+^2 \bar{m}_\phi^2 \right]. \quad (17)$$

It is worth stressing that the derivatives in eqs. (16) and (17) are with respect to  $x$ , i.e.,  $d/dx$ .

### 2.3. Solutions at the vicinity of the event horizon

Our first solution regarding eqs. (16) and (17) is valid for  $\rho$  in a small vicinity of  $\rho_+$ , with  $\rho_+ \neq 0$ . In this case, we considered the first-order approximation for (8) according to which

$$A(x) = \beta_+ (x - 1) . \quad (18)$$

where

$$\beta_+ = \frac{2\rho_+^2}{l^2} + \frac{\rho_s}{\rho_+} + 2\alpha_q N_q \rho_+^{2\alpha_q} , \quad (19)$$

implying  $\beta_+ > 0$ . We required  $\rho_s \neq 0$  to promote the necessary condition  $\rho_+ \neq 0$ . The solution of the radial wave function  $R(x)$  for the scalar particle, following eqs. (12) and (16)–(18), is given by

$$R(x) = x^{(\beta-1)/2} (x-1)^{\gamma/2} [c_1 \text{HeunC}(\alpha, \beta, \gamma, \delta, \eta; x) + c_2 x^{-\beta} \text{HeunC}(\alpha, -\beta, \gamma, \delta, \eta; x)] , \quad (20)$$

where  $\text{HeunC}(\alpha, \beta, \gamma, \delta, \eta; x)$  is the confluent Heun function [40, 51]. The Heun parameters  $\alpha, \beta, \gamma, \delta$ , and  $\eta$  are

$$\begin{aligned} \alpha &= 0 , \\ \beta &= \pm \sqrt{1 - \frac{4\kappa^2}{\beta_+}} , \\ \gamma &= \pm i \frac{2\epsilon\rho_+}{\beta_+} , \\ \delta &= -\frac{\rho_+^2 \bar{m}_\phi^2}{\beta_+} , \\ \eta &= -\frac{1}{2} - \frac{\kappa^2}{\beta_+} . \end{aligned} \quad (21)$$

The above solution is valid only for a small region where  $|x-1| \approx 0$ . That is, we cannot go far away from the event horizon. That being established, it follows from eq. (A.39) that the confluent Heun function can be simplified around  $x=1$ , where  $\text{HeunC}(\alpha, \pm\beta, \gamma, \delta, \eta; x) \approx 1$ . By analyzing the limit  $\lim_{x \rightarrow 1} R(x)$ , we obtain that:

$$R(x) = c_1 \exp \left[ \frac{\gamma}{2} \ln(x-1) + \frac{\beta}{2} (x-1) \right] + c_2 \exp \left[ \frac{\gamma}{2} \ln(x-1) - \frac{\beta}{2} (x-1) \right] . \quad (22)$$

Unless  $\beta \gg \gamma$ , the dominant term in  $R(x)$  for  $x \rightarrow 1^+$  behaves as

$$R(x) \propto (x - 1)^{\gamma/2}, \quad (23)$$

up to a multiplicative constant. Thus, considering the expression for  $\gamma$  shown in (21), the real part of  $R(x)$  behaves as  $\cos\left[\frac{\epsilon\rho_+}{\beta_+} \ln(x - 1) + \theta_0\right]$ , where  $\theta_0$  is an arbitrary phase. This suggests that the radial wave function oscillates rapidly near the event horizon.

Although the solution given by (20) is important, it is valid only when  $|x - 1| \approx 0$ , i.e., on a small vicinity of  $\rho_+$ . In this work, however, we are interested in solutions where the scalar particle can be at varying distances  $\rho$  from  $\rho_+$ . To do so, we consider one single assumption: that  $\rho$  and  $\rho_+$  are significantly smaller than the AdS radius  $|l|$ , implying that  $\rho^2 \ll l^2$  is negligible in (8). This assumption means that, as long as  $\alpha_q \neq 1$ , we are considering particles in a large extended domain, but not at a cosmological scale. Under this condition, we see that  $A(\rho)$  becomes

$$A(\rho) = \bar{a} - \frac{\rho_s}{\rho} + N_q \rho^{2\alpha_q}. \quad (24)$$

Conversely, when  $\alpha_q = 1$ , we can investigate the whole radial domain because the combined contribution of  $N_q$  and  $1/l^2$  facilitate the analysis, as will be detailed in section 5.

Therefore, we investigate the solutions of the radial Klein-Gordon equation for some fixed values of  $\alpha_q$ , namely  $\alpha_q = 0, 1/2, 1$ . For clarity, we shall label these solutions with a descriptive subindex from table 4 so that, given the label, we can easily identify the conditions leading to it. To explicitly

Index	Meaning	Conditions on $\bar{a}$ , $\rho_s$ , and $N_q$
ST	Standard case	All parameters non-zero
CL	Cloudless	$\bar{a} = 0, \rho_s \neq 0$
HL	Horizonless	$\rho_s = 0$
F	Free from quintessence	$N_q = 0$

Table 4: Labels for the extended solutions.

indicate the value of the state parameter  $\alpha_q$  associated with each solution, we employ an upper index notation. For instance,  $R_{ST}^{(1/2)}(x)$  represents the radial wave function for the standard case (meaning  $\bar{a} \neq 0, \rho_s \neq 0$ , and  $N_q \neq 0$ ) for  $\alpha_q = 1/2$ .

We shall discuss such solutions in the forthcoming sections, beginning with the case of  $\alpha_q = 0$ , which we call lower bound.

### 3. Lower bound for the state parameter

As evident from eq. (4), the Kiselev quintessence fluid is characterized by the parameter  $\alpha_q$ . Consequently, we expect that the behavior of the scalar particles will be influenced by the value considered for this parameter. Motivated by this, we explored this effect by solving the Klein-Gordon equation for various  $\alpha_q$  values and across different scenarios determined by the theory's other parameters.

To begin our investigation, we first consider the case where  $\alpha_q = 0$ , corresponding to  $\omega_q = -1/3$ . This limit represents the maximum contribution of quintessence to  $A(\rho)$ . In this regime, its effect is indistinguishable from that of the string clouds. Then, using the expression from eq. (24), we can write:

$$A(\rho) = (\bar{a} + N_q) - \frac{\rho_s}{\rho}.$$

Given that

$$\rho_+ = \frac{\rho_s}{\bar{a} + N_q},$$

where  $\bar{a} \neq 0$ ,  $N_q \neq 0$ , and  $\rho_s \neq 0$ , we have:

$$A(x) = (\bar{a} + N_q) \left(1 - \frac{1}{x}\right). \quad (25)$$

Substituting the result from eq. (25) into the effective potential (17) yields

$$\rho_+^2 V_{\text{eff}}(x) = \frac{1/4}{x^2(x-1)^2} + \left(\frac{\epsilon \rho_+^2}{\rho_s}\right)^2 \frac{x^2}{(x-1)^2} - \kappa^2 \frac{\rho_+/\rho_s}{x(x-1)} - \frac{\rho_+^3 \bar{m}_\phi^2}{\rho_s} \frac{x}{x-1}. \quad (26)$$

To rewrite  $\rho_+^2 V_{\text{eff}}(x)$  in a more convenient way, we introduce the following definitions

$$\begin{aligned} \epsilon_0 &= \frac{\epsilon \rho_+^2}{\rho_s} = \frac{\epsilon \rho_s}{(\bar{a} + N_q)^2}, \\ \kappa_0^2 &= \frac{\kappa^2 \rho_+}{\rho_s} = \frac{\kappa^2}{(\bar{a} + N_q)}, \\ m_0^2 &= \frac{\bar{m}_\phi^2 \rho_+^3}{\rho_s} = \frac{\bar{m}_\phi^2 \rho_s^2}{(\bar{a} + N_q)^3}, \end{aligned} \quad (27)$$

and then, performing a partial fraction decomposition of eq. (26), we can express the effective potential as

$$\rho_+^2 V_{\text{eff}}(x) = \frac{\kappa_0^2 + 1/2}{x} + \frac{1/4}{x^2} + \frac{2\epsilon_0^2 - \kappa_0^2 - m_0^2 - 1/2}{x-1} + \frac{\epsilon_0^2 + 1/4}{(x-1)^2} + (\epsilon_0^2 - m_0^2). \quad (28)$$

Comparing (16) and (28) with the normal form of the confluent Heun equation, given by eqs. (A.15) and (A.16), we find that

$$u_{ST}^{(0)}(x) = u_0 x^{1/2} (x-1)^{(1+\gamma)/2} e^{\alpha x/2} \text{HeunC}(\alpha, \beta, \gamma, \delta, \eta; x), \quad (29)$$

where the subscript  $ST$  denotes the standard case, as defined in table 4, and the superscript (0) indicates  $\alpha_q = 0$ . The parameters of the confluent Heun function are

$$\begin{aligned} \alpha &= \pm 2\sqrt{m_0^2 - \epsilon_0^2}, \\ \beta &= 0, \\ \gamma &= \pm 2i\epsilon_0, \\ \delta &= 2\epsilon_0^2 - m_0^2, \\ \eta &= -\kappa_0^2. \end{aligned} \quad (30)$$

The solution (29) simplifies significantly compared to (A.17) due to  $\beta = 0$  in eq. (30).

Combining eqs. (12), (25) and (29), we obtain that the formal solution for the radial wave function  $R_{ST}^{(0)}(x)$  is

$$R_{ST}^{(0)}(x) = R_0 (x-1)^{\gamma/2} e^{\alpha x/2} \text{HeunC}(\alpha, \beta, \gamma, \delta, \eta; x). \quad (31)$$

This solution, corresponding to  $\alpha_q = 0$ , is valid for  $\rho = x\rho_+$  provided that  $\rho \ll |l|$ . For example, with  $|l| = 3.8 \times 10^{26}$  m,  $N_q = 8.95$ ,  $\bar{a} = 10^{-4}$ , and  $\rho_s = 10^{10}$  m, we calculate  $\rho_+ \approx 1.12 \times 10^9$  m. Consequently, the approximation for  $A(x)$  remains valid up to  $10^{14}$  times the event horizon radius. This contrasts with the solution described by (21), which is valid only for  $|x-1| \approx 0$ .

Finally, if we impose the constraint of eq. (A.42) to require the local<sup>1</sup> confluent Heun function to be truncated into a polynomial, we would obtain

---

<sup>1</sup>Remember that the radius of convergence for the confluent Heun function is of one unit, according to the Frobenius method [49].

that the quantum energy levels  $\epsilon$ , present in eq. (27), should satisfy

$$N + 1 \pm i\epsilon_0 = \pm \frac{m_0^2 - 2\epsilon_0^2}{2\sqrt{m_0^2 - \epsilon_0^2}}, \quad (32)$$

with  $N \in \mathbb{Z}$ . However, this result does not imply that all energy eigenstates are given by the above result. It only shows that, as long as the local confluent Heun function becomes a polynomial, these energy levels are determined by eq. (32).

In the subsequent section, we will demonstrate that the solution (31) and the constraint (32) exhibit only minor variations when string clouds are absent.

### 3.1. Special case without the string clouds

The radial wave function for the cloudless scenario,  $R_{CL}^{(0)}(x)$ , is directly obtained from (31) by setting  $\bar{a} = 0$ . In this case,  $R_{CL}^{(0)}(x)$  depends only on the quintessence parameter  $N_q$  and the Schwarzschild-like radius  $\rho_s$ . Therefore, the parameters (27) occurring in  $R_{ST}^{(0)}(x)$  simplify to the following, where the subscript  $CL$  denotes the cloudless case, as defined in table 4:

$$\epsilon_{CL}^{(0)} = \frac{\epsilon\rho_s}{N_q^2}, \quad \kappa_{CL}^{(0)} = \sqrt{\frac{\kappa^2}{N_q}}, \quad m_{CL}^{(0)} = \sqrt{\frac{\bar{m}_\phi^2 \rho_s^2}{N_q^3}}.$$

Notably, this cloudless scenario closely resembles the standard general case of  $\alpha_q = 0$  because, as mentioned earlier, string clouds and quintessence exhibit identical behavior in this limiting case.

In the next subsection, we show the consequences of removing the black string and how this first horizonless scenario behaves.

### 3.2. Removing the black string

The third possible solution when  $\alpha_q = 0$  is the one where  $\rho_s = 0$ , while  $\bar{a}$  and/or  $N_q$  are nontrivial. This condition implies that  $A(\rho)$ , given by eq. (24), becomes simply

$$A(\rho) = \bar{a} + N_q, \quad (33)$$

provided that  $\rho \ll |l|$ , allowing us to neglect the  $\rho^2/l^2$  term in (8). Since  $\rho_s = 0$  eliminates the event horizon, we express  $A(\rho)$  in terms of  $\rho$  rather

than  $x = \rho/\rho_+$ . Hence, substituting eq. (33) into eq. (14) yields the effective potential:

$$V_{\text{eff}}(\rho) = \frac{\epsilon^2}{(\bar{a} + N_q)^2} - \frac{\bar{m}_\phi^2}{(\bar{a} + N_q)} - \frac{\kappa^2/(\bar{a} + N_q)}{\rho^2}. \quad (34)$$

Considering the differential equation for  $u(\rho)$ , defined by eq. (16), the effective potential (34) above, and the general result of eq. (A.15), we obtain that the solution for  $u_{\text{HL}}^{(0)}(\rho)$  is given by

$$u_{\text{HL}}^{(0)}(\rho) = e^{\alpha\rho/2} \rho^{(1+\beta)/2} (\rho - 1)^{(1+\gamma)/2} [c_1 \text{HeunC}(\alpha, \beta, \gamma, \delta, \eta; \rho) + c_2 \rho^{-\beta} \text{HeunC}(\alpha, -\beta, \gamma, \delta, \eta; \rho)], \quad (35)$$

where the subindex “HL” stands for “horizonless”, in accordance with table 4. The Heun parameters are:

$$\begin{aligned} \alpha &= \pm \frac{2i}{\bar{a} + N_q} \sqrt{\epsilon^2 - (\bar{a} + N_q) \bar{m}_\phi^2}, \\ \beta &= \pm 2 \sqrt{\frac{1}{4} + \frac{\kappa^2}{\bar{a} + N_q}}, \\ \gamma &= \pm 1, \\ \delta &= 0, \\ \eta &= \frac{1}{2}. \end{aligned} \quad (36)$$

Thus, the complete solution describing the radial wave function  $R_{\text{HL}}^{(0)}(\rho)$  is:

$$R_{\text{HL}}^{(0)}(\rho) = e^{\alpha\rho/2} \rho^{(\beta-1)/2} (\rho - 1)^{(1+\gamma)/2} [c_1 \text{HeunC}(\alpha, \beta, \gamma, \delta, \eta; \rho) + c_2 \rho^{-\beta} \text{HeunC}(\alpha, -\beta, \gamma, \delta, \eta; \rho)], \quad (37)$$

where  $c_1$  and  $c_2$  are constants. In case we apply the constraint from (A.30), to require  $\text{HeunCl}(\alpha, \beta, \gamma, \delta, \eta; \rho)$  to be a polynomial, we obtain the following restrictions:

$$\epsilon^2 = \bar{m}_\phi^2 (\bar{a} + N_q),$$

and

$$N + 1 \pm \frac{1}{2} \left( 1 + \sqrt{\frac{1}{4} + \frac{\kappa^2}{\bar{a} + N_q}} \right) = 0.$$

As an alternative to the use of the confluent Heun function, we can solve eq. (13) with the particular case of the effective potential (34) as a Bessel equation. This leads to the solution:

$$u_{\text{HL}}^{(0)}(\rho) = \rho^{1/2} [c_1 J_m(k\rho) + c_2 Y_m(k\rho)] , \quad (38)$$

where  $J_m(x)$  and  $Y_m(x)$  are the  $m$ -th order Bessel functions of the first and second kinds,  $c_1$  and  $c_2$  are constants, and

$$k = \frac{\epsilon^2}{(\bar{a} + N_q)^2} - \frac{\bar{m}_\phi^2}{(\bar{a} + N_q)} , \quad (39)$$

$$m = \sqrt{\frac{1}{4} + \frac{\kappa^2}{\bar{a} + N_q}} . \quad (40)$$

The properties of Bessel functions are described in detail in [51, 49, 50].

Using eq. (12), the radial wave function  $R_{\text{HL}}^{(0)}(\rho)$  becomes:

$$R_{\text{HL}}^{(0)}(\rho) = \rho^{-1/2} [c_1 J_m(k\rho) + c_2 Y_m(k\rho)] . \quad (41)$$

When  $m > 1/2$ , corresponding to  $\kappa^2 \neq 0$ , we set  $c_2 = 0$  to guarantee a non-singular wave function near the origin.

### 3.3. In the absence of quintessence

We now examine the solution for  $N_q = 0$ , with  $\bar{a} \neq 0$  and  $\rho_s \neq 0$ , regardless of the value of  $\alpha_q$ . We maintain the assumption that  $\rho \ll |l|$ , thus neglecting  $\rho^2/l^2$ . Furthermore, this solution is a valid approximation for  $\alpha_q > 1/2$  when the terms  $\rho^2/l^2 + N_q \rho^{2\alpha_q}$  are infinitely small compared to  $\bar{a} - \rho_s/\rho$ . Under these assumptions,  $A(x)$  simplifies to

$$A(x) = \bar{a} - \frac{\rho_s}{\rho_+} \frac{1}{x} .$$

Since

$$\rho_+ = \frac{\rho_s}{\bar{a}} ,$$

we obtain

$$A(x) = \bar{a} \left( 1 - \frac{1}{x} \right) . \quad (42)$$

Notably, eq. (42) has the exact same form of (25), with the substitution of  $N_q + \bar{a}$  by  $\bar{a}$ . Consequently, the effective potential (28) becomes

$$\rho_+^2 V_{\text{eff}}(x) = \frac{\kappa_F^2 + 1/2}{x} + \frac{1/4}{x^2} + \frac{2\epsilon_F^2 - \kappa_F^2 - m_F^2 - 1/2}{x-1} + \frac{\epsilon_F^2 + 1/4}{(x-1)^2} + (\epsilon_F^2 - m_F^2), \quad (43)$$

where the subscript “ $F$ ” indicates the absence of quintessence. The parameters  $\epsilon_F$ ,  $\kappa_F$ , and  $m_F$  follow from eq. (27) :

$$\epsilon_F = \frac{\epsilon \rho_S}{\bar{a}^2}, \quad \kappa_F = \frac{\kappa}{\bar{a}^{1/2}}, \quad m_F = \frac{\rho_S \bar{m}_\phi}{\bar{a}^{3/2}}. \quad (44)$$

Using the differential equation (16) with the effective potential (43), we find that  $u_F(x)$  has the same form as (29), with

$$\begin{aligned} \alpha &= \pm 2i \frac{\rho_S}{\bar{a}^2} \sqrt{\epsilon^2 - \bar{a} \bar{m}_\phi^2}, \\ \beta &= 0, \\ \gamma &= \pm 2i \frac{\epsilon \rho_S}{\bar{a}^2}, \\ \delta &= \frac{2\rho_S^2}{\bar{a}^4} \left( \epsilon^2 - \frac{1}{2} \bar{a} \bar{m}_\phi^2 \right), \\ \eta &= -\frac{\kappa^2}{\bar{a}}. \end{aligned} \quad (45)$$

Therefore, the radial wave function  $R_F(x)$  is

$$R_F(x) = R_0 (x-1)^{\gamma/2} e^{\alpha x/2} \text{HeunC}(\alpha, \beta, \gamma, \delta, \eta; x). \quad (46)$$

Although we have a large domain for  $x$ , if  $x \rightarrow 1^+$ ,  $R_F(x)$  behaves as

$$R_F(x) \propto (x-1)^{\gamma/2} e^{\alpha/2}. \quad (47)$$

In the special case where  $1 < x < 2$ , so that the local solution to the confluent Heun equation holds, we may impose the constraint from (A.30), which requires  $\text{HeunC}\ell(\alpha, \beta, \gamma, \delta, \eta; x)$  to be a polynomial. Under this condition:

$$N + 1 \pm i \frac{\epsilon \rho_S}{\bar{a}^2} = \pm \frac{\rho_S}{\bar{a}^2} \left( \epsilon^2 - \frac{1}{2} \bar{a} \bar{m}_\phi^2 \right) \frac{1}{\sqrt{\epsilon^2 - \bar{a} \bar{m}_\phi^2}}.$$

It is important to emphasize that the above result does not encompass all possible energy levels.

Having examined all cases for  $\alpha_q = 0$ , we now turn to the physically significant case of  $\alpha_q = 1/2$ . This midpoint value corresponds to a scenario where the quintessence's influence on the metric is only significant at large distances.

#### 4. Solutions for the intermediate state parameter

To examine the implications of a scalar particle within this spacetime, with  $\alpha_q = 1/2$  ( $\omega_q = -2/3$ ), let us consider eq. (24). The event horizon  $\rho_+$  satisfies

$$\bar{a} - \frac{\rho_s}{\rho_+} + N_q \rho_+ = 0, \quad (48)$$

under the approximation  $\rho_+^2 \ll l^2$ . For any value of  $N_q$ ,  $A(x)$  can be expressed as

$$A(x) = \bar{a} - \frac{\rho_s}{\rho_+} \frac{1}{x} + N_q \rho_+ x,$$

provided  $\rho_+ \neq 0$ , which requires  $\rho_s \neq 0$ . Using the constraint from eq. (48), we can rewrite the above expression for  $A(x)$  as

$$A(x) = \bar{a} \left(1 - \frac{1}{x}\right) \left[1 + \frac{N_q \rho_+}{\bar{a}} (1 + x)\right]. \quad (49)$$

Moreover, it follows directly from eq. (48) that

$$\frac{N_q \rho_+}{\bar{a}} = \frac{1}{2} \left( \sqrt{1 + \frac{4 N_q \rho_s}{\bar{a}^2}} - 1 \right),$$

and given the ranges of  $\bar{a}$ ,  $\rho_s$ , and  $N_q$  presented in section 2, it is reasonable to consider solutions satisfying

$$\frac{N_q \rho_s}{\bar{a}^2} \ll 1, \quad (50)$$

so that

$$\frac{N_q \rho_+}{\bar{a}} = \frac{N_q \rho_s}{\bar{a}^2} + \mathcal{O}\left(\frac{N_q \rho_s}{\bar{a}^2}\right)^2.$$

In this regime, eq. (49) becomes

$$A(x) = \bar{a} \left(1 - \frac{1}{x}\right) \left[1 + \frac{N_q \rho_s}{\bar{a}^2} (1 + x)\right], \quad (51)$$

which represents a first-order correction to the case where quintessence is absent, given by eq. (42). Notably, this correction increases with  $x$ , indicating that dark energy's influence becomes significant at large distances.

From eq. (51), the derivatives  $A'(x)$  and  $A''(x)$  are:

$$A'(x) = \frac{\bar{a}}{x^2} \left[ 1 + \frac{N_q \rho_s}{\bar{a}^2} (1 + x^2) \right], \quad (52)$$

$$A''(x) = -\frac{2\bar{a}}{x^3} \left( 1 + \frac{N_q \rho_s}{\bar{a}^2} \right). \quad (53)$$

In the sequence, we use eqs. (51)–(53) to explicitly determine the effective potential  $\rho_+^2 V_{\text{eff}}(x)$ , given by eq. (17) in the regime of eq. (50). For convenience, we give the results in their partial fraction decompositions:

$$\frac{A'(x)^2}{4A(x)^2} = \frac{(1 - N_q \rho_s / \bar{a}^2) / 2}{x} + \frac{1/4}{x^2} - \frac{(1 - N_q \rho_s / \bar{a}^2) / 2}{x - 1} + \frac{1/4}{(x - 1)^2}, \quad (54a)$$

$$\begin{aligned} \frac{\rho_+^2 \epsilon^2}{A(x)^2} &= \left( \frac{\epsilon \rho_s}{\bar{a}^2} \right)^2 \left[ \frac{2 - 10 N_q \rho_s / \bar{a}^2}{x - 1} + \frac{1 - 4 N_q \rho_s / \bar{a}^2}{(x - 1)^2} + \left( 1 - \frac{6 N_q \rho_s}{\bar{a}^2} \right) \right. \\ &\quad \left. - \frac{2 N_q \rho_s}{\bar{a}^2} x \right], \end{aligned} \quad (54b)$$

as well as

$$-\frac{1}{A(x)} \left[ \frac{1}{2} A''(x) + \frac{A'(x)}{x} \right] = -\frac{N_q \rho_s / \bar{a}^2}{x - 1}, \quad (54c)$$

and

$$-\frac{\kappa^2}{x^2 A(x)} = \frac{\kappa^2 / \bar{a} (1 - N_q \rho_s / \bar{a}^2)}{x} - \frac{\kappa^2 / \bar{a} (1 - 2 N_q \rho_s / \bar{a}^2)}{x - 1}, \quad (54d)$$

$$-\frac{\rho_+^2 \bar{m}_\phi^2}{A(x)} = -\left( \frac{\rho_s \bar{m}_\phi}{\bar{a}^{3/2}} \right)^2 \left[ \frac{1 - 2 N_q \rho_s / \bar{a}^2}{x - 1} + \left( 1 - \frac{2 N_q \rho_s}{\bar{a}^2} \right) - \frac{N_q \rho_s}{\bar{a}^2} x \right]. \quad (54e)$$

After adding eqs. (54a)–(54e), we conclude that the effective potential (17) can be written as

$$\rho_+^2 V_{\text{eff}}(x) = \frac{A}{x} + \frac{B}{x - 1} + \frac{C}{x^2} + \frac{D}{(x - 1)^2} + E + F x, \quad (55)$$

with

$$A = \left( \frac{1}{2} + \frac{\kappa^2}{\bar{a}} \right) \left( 1 - \frac{N_q \rho_s}{\bar{a}^2} \right), \quad (56a)$$

$$B = -\frac{1}{2} \left( 1 + \frac{N_q \rho_s}{\bar{a}^2} \right) - \frac{1}{\bar{a}} \left( \kappa^2 + \frac{\rho_s^2 \bar{m}_\phi^2}{\bar{a}^2} \right) \left( 1 - \frac{2 N_q \rho_s}{\bar{a}^2} \right) + 2 \left( \frac{\epsilon \rho_s}{\bar{a}^2} \right)^2 \left( 1 - \frac{5 N_q \rho_s}{\bar{a}^2} \right), \quad (56b)$$

$$C = \frac{1}{4}, \quad (56c)$$

$$D = \frac{1}{4} + \left( \frac{\epsilon \rho_s}{\bar{a}^2} \right)^2 \left( 1 - \frac{4 N_q \rho_s}{\bar{a}^2} \right) \quad (56d)$$

$$E = \left( \frac{\epsilon \rho_s}{\bar{a}^2} \right)^2 \left( 1 - \frac{6 N_q \rho_s}{\bar{a}^2} \right) - \frac{1}{\bar{a}} \frac{\rho_s^2 \bar{m}_\phi^2}{\bar{a}^2} \left( 1 - \frac{2 N_q \rho_s}{\bar{a}^2} \right) \quad (56e)$$

$$F = \frac{N_q \rho_s^3}{\bar{a}^5} \left( \bar{m}_\phi^2 - \frac{2\epsilon^2}{\bar{a}} \right). \quad (56f)$$

Comparing eqs. (56a)–(56f) with eqs. (43) and (44) reveals that the effective potential at the midpoint of the interval represents a first-order adjustment to the scenario where quintessence is absent. Furthermore, in the limit  $N_q \rho_s / \bar{a}^2 \rightarrow 0$ , eqs. (56a)–(56f) reduce to the case of eq. (43).

Although the term  $F$ , defined in (56f), presents a new difficulty to the solution, we can consider the special case where  $F = 0$ , leading to

$$\epsilon^2 = \frac{1}{2} \bar{a} \bar{m}_\phi^2, \quad (57)$$

and with this procedure obtain a solution which presents the main features of the system. This constraint simplifies the coefficients (56b) and (56e) to

$$\bar{B} = -\frac{1}{2} \left( 1 + \frac{N_q \rho_s}{\bar{a}^2} \right) - \frac{\kappa^2}{\bar{a}} \left( 1 - \frac{2 N_q \rho_s}{\bar{a}^2} \right) - 6 \left( \frac{\epsilon \rho_s}{\bar{a}^2} \right)^2 \frac{N_q \rho_s}{\bar{a}^2}, \quad (58a)$$

$$\bar{E} = - \left( \frac{\epsilon \rho_s}{\bar{a}^2} \right)^2 \left( 1 + \frac{2 N_q \rho_s}{\bar{a}^2} \right), \quad (58b)$$

while (56a), (56c), and (56d) remain unchanged. Given the constraint of eq. (57), the solution for  $\alpha_q = 1/2$  can be expressed in terms of the confluent Heun equation:

$$u_{ST}^{(1/2)}(x) = x^{(1+\beta)/2} (x-1)^{(1+\gamma)/2} e^{\alpha x/2} \text{HeunC}(\alpha, \beta, \gamma, \delta, \eta; x), \quad (59)$$

where the Heun parameters are

$$\begin{aligned}
\alpha &= \pm 2 \frac{\epsilon \rho_s}{\bar{a}^2} \sqrt{1 + \frac{2 N_q \rho_s}{\bar{a}^2}}, \\
\beta &= 0, \\
\gamma &= \pm 2i \frac{\epsilon \rho_s}{\bar{a}^2} \sqrt{1 - \frac{4 N_q \rho_s}{\bar{a}^2}}, \\
\delta &= -\frac{N_q \rho_s}{\bar{a}^2} \left( 1 - \frac{\kappa^2}{\bar{a}} + 6 \frac{\epsilon^2 \rho_s^2}{\bar{a}^4} \right), \\
\eta &= \frac{N_q \rho_s}{\bar{a}^2} \left( \frac{1}{2} + \frac{\kappa^2}{\bar{a}} \right) - \frac{\kappa^2}{\bar{a}}.
\end{aligned} \tag{60}$$

Using the relation between  $u_{st}^{(1/2)}(x)$  and  $R_{st}^{(1/2)}(x)$ , determined by eq. (12), we conclude that:

$$R_{st}^{(1/2)}(x) = R_0 \left[ 1 - \frac{1}{2} \frac{N_q \rho_s}{\bar{a}^2} (1+x) \right] (x-1)^{\gamma/2} e^{\alpha x/2} \text{HeunC}(\alpha, \beta, \gamma, \delta, \eta; x), \tag{61}$$

where  $A(x)^{-1/2}$  has been approximated to first order in  $N_q \rho_s / \bar{a}^2$ .

Imposing the energy constraint of eq. (57) to the solution described by eq. (45) yields the result of eq. (60) in the limit  $N_q \rho_s / \bar{a}^2 \rightarrow 0$ . This equivalence arises because, under these constraints, both solutions describe the same physical background.

Finally, it should be clear that for the radial wave function determined by eq. (61), we shall not impose the constraint for polynomial solutions since we have imposed the energy condition (57) to obtain a special solution in terms of the confluent Heun function. The situation will be different in the next section, where we shall consider the cloudless scenario keeping  $\alpha_q = 1/2$ .

#### 4.1. Middle of the interval: cloudless regime

We now consider the cloudless regime where  $\alpha_q = 1/2$  (corresponding to  $\omega_q = -2/3$ ). Applying the constraint from eq. (48), we obtain

$$\rho_+ = \left( \frac{\rho_s}{N_q} \right)^{1/2}. \tag{62}$$

Based on the admissible values for  $\rho_s$  and  $N_q$  established in section 2, the condition  $\rho_+ \ll |l|$  remains valid, and this is true because we considered a

large universe with  $\rho_{obs.} \sim |l| \sim 10^{26}$  m. In this situation, the metric function  $A(x)$  simplifies to

$$A(x) = (N_q \rho_s)^{1/2} \left( x - \frac{1}{x} \right), \quad (63)$$

with  $(N_q \rho_s)^{1/2}$  ranging from  $10^{-14}$  to  $10^{-5}$  (approximately). The above expression for  $A(x)$  indicates that, unless  $x$  is small, such as  $1 < x < 4$  for instance, a good approximation for eq. (63) is

$$A(x) = (N_q \rho_s)^{1/2} x. \quad (64)$$

Previously, the spin-0 particle's behavior near the event horizon was analyzed using eqs. (20), (21) and (23) with  $\beta_+ = 2(N_q \rho_s)^{1/2}$ . We now extend our investigation to the regime where the approximation in eq. (64) is valid.

Substituting the approximate metric function  $A(x)$  from eq. (64) into the general expression of 17, we derive an effective potential of the form

$$\rho_+^2 V_{\text{eff}}(x) = -\frac{\overline{m}_\phi^2 \rho_s^{1/2}}{N_q^{3/2}} \frac{1}{x} + \left( \frac{\epsilon^2}{N_q^2} - \frac{3}{4} \right) \frac{1}{x^2} - \frac{\kappa^2}{(N_q \rho_s)^{1/2}} \frac{1}{x^3}. \quad (65)$$

Observe that each term in eq. (65) scales with a power of  $N_q^{-1}$ . To analyze the relative magnitudes of the  $x^{-3}$  and  $x^{-1}$  terms, we compute their ratio:

$$\frac{\kappa^2 / (N_q \rho_s)^{1/2}}{\overline{m}_\phi^2 \rho_s^{1/2} / N_q^{3/2}} = \frac{N_q}{\rho_s} \left( \frac{\kappa^2}{\overline{m}_\phi^2} \right), \quad (66)$$

where the ratio  $N_q/\rho_s$  typically ranges from  $10^{-24}$  m<sup>2</sup> to  $10^{-41}$  m<sup>2</sup>. Since  $\kappa^2 = n_R^2 + k_z^2$ , with  $n_R \in \mathbb{Z}$  and  $k_z^2 \propto \overline{m}_\phi^2$ , the contribution of the  $x^{-3}$  term in (65) is negligible compared to the  $x^{-1}$  term. Consequently, we can approximate eq. (16) by considering only the first two terms of eq. (65). The resulting solution for  $u_{CL}^{(1/2)}(x)$  can then be expressed in terms of the confluent Heun function as

$$u_{CL}^{(1/2)}(x) = x^{(1+\beta)/2} (x-1)^{(1+\gamma)/2} [c_1 \text{HeunC}(\alpha, \beta, \gamma, \delta, \eta; x) + c_2 x^{-\beta} \text{HeunC}(\alpha, -\beta, \gamma, \delta, \eta; x)], \quad (67)$$

with the Heun parameters being

$$\begin{aligned}
\alpha &= 0, \\
\beta &= \pm 2 \sqrt{1 - \frac{\epsilon^2}{N_q^2}}, \\
\gamma &= \pm 1, \\
\delta &= \frac{1}{2} + \frac{\overline{m}_\phi^2 \rho_s^{1/2}}{N_q^{3/2}}, \\
\eta &= -\frac{\overline{m}_\phi^2 \rho_s^{1/2}}{N_q^{3/2}}.
\end{aligned} \tag{68}$$

The radial wave function, given by eq. (12), takes the form:

$$\begin{aligned}
R_{CL}^{(1/2)}(x) &= x^{(\beta-2)/2} (x-1)^{(1+\gamma)/2} \left[ c_1 \text{HeunC}(\alpha, \beta, \gamma, \delta, \eta; x) \right. \\
&\quad \left. + c_2 x^{-\beta} \text{HeunC}(\alpha, -\beta, \gamma, \delta, \eta; x) \right],
\end{aligned} \tag{69}$$

where the Heun parameters are specified in eq. (68). Since the parameter  $\alpha$  is zero and  $\delta > 0$ , we cannot impose the constraint (A.30) in this case. Thus, in principle, the energy eigenstates are not restricted in this scenario.

An equivalent solution is obtained when we solve eq. (13), with the effective potential (65), in terms of Bessel's functions:

$$u_{CL}^{(1/2)}(x) = x^{1/2} \left[ c_1 I_s(2\sqrt{bx}) + c_2 K_s(2\sqrt{bx}) \right], \tag{70}$$

where  $I_s(x)$  and  $K_s(x)$  are the modified Bessel functions of the first and second kinds, respectively. The scale factor  $b$  and the order  $s$  are determined by

$$b = \frac{\overline{m}_\phi^2 \rho_s^{1/2}}{N_q^{3/2}}, \tag{71}$$

$$s = 2 \sqrt{1 - \frac{\epsilon^2}{N_q^2}}. \tag{72}$$

Note that, with  $N_s \neq 0$ , it becomes clear that  $b$  is a real positive number, while  $s$  is purely imaginary (unless  $\epsilon = 0$ ). In this convenient format, the radial wave function takes the form of

$$R_{CL}^{(1/2)}(x) = x^{-1} \left[ c_1 I_s(2\sqrt{bx}) + c_2 K_s(2\sqrt{bx}) \right]. \tag{73}$$

*Extra cases:*

For the special case of a massless scalar field ( $\bar{m}_\phi = 0$ ), the situation gets simpler, and the dominant term in the effective potential (65) becomes

$$\rho_+^2 V_{\text{eff}}(x) = \left( \frac{\epsilon^2}{N_q^2} - \frac{3}{4} \right) \frac{1}{x^2}.$$

Although we could write the solution in terms of the confluent Heun function, it is simpler to give the solution as

$$u_{CL}^{(1/2, \Delta)}(x) = x^{1/2} \left[ c_1 x^{s/2} + c_2 x^{-s/2} \right], \quad (74)$$

with  $s$  defined by eq. (72). Since  $s$  is purely imaginary, the real part of this solution behaves as  $\text{Re} [u_{CL}^{(1/2, \Delta)}(x)] \propto x^{1/2} \cos\left(\frac{s}{2} \ln x\right)$  (if setting  $c_1$  or  $c_2$  to zero, for simplicity).

On the other hand, in the particular case where  $\epsilon^2 = 3 N_q^2/4$ , with  $\bar{m}_\phi \neq 0$ , the effective potential (65) reduces to:

$$\rho_+^2 V_{\text{eff}}(x) = -\frac{\bar{m}_\phi^2 \rho_s^{1/2}}{N_q^{3/2}} \frac{1}{x},$$

and the solution to eq. (13) is:

$$u_{CL}^{(1/2, \square)}(x) = \sqrt{bx} \left[ c_1 I_1(2\sqrt{bx}) + c_2 K_1(2\sqrt{bx}) \right], \quad (75)$$

where  $b$  is given by eq. (71).

The corresponding radial wave functions for these two special cases, (74) and (75), are obtained via:

$$R_{CL}^{(1/2, \Delta/\square)}(x) = x^{-1} u_{CL}^{(1/2, \Delta/\square)}(x). \quad (76)$$

We stress that the constants  $c_1$  and  $c_2$  absorbed any normalization constant  $R_0$  in eq. (76).

The remaining scenario with  $\alpha_q = 1/2$  involves removing the black string, i.e., setting  $\rho_s = 0$ . This will be explored in the next subsection.

#### 4.2. Intermediate Case: Absence of Schwarzschild-like Radius

We now examine the particle wave function in the absence of black strings ( $\rho_s = 0$ ), while keeping the quintessence state parameter at  $\alpha_q = 1/2$  and

the condition  $\rho \ll |l|$ , which means a system with mass, due to the cloud of strings, and quintessence. Under these assumptions, the metric function simplifies to:

$$A(\rho) = \bar{a} \left( 1 + \frac{N_q}{\bar{a}} \rho \right). \quad (77)$$

Recall that, in this regime, the physical values of  $N_q/\bar{a}$  typically range from  $10^{-20}$  to  $10^{-27} \text{ m}^{-1}$ . Consequently, we retain only the first-order approximations in  $N_q/\bar{a}$  when deriving the effective potential given by eq. (14). This approach mirrors the procedure in section 4, albeit with a simplified form in the present case. The resulting effective potential is:

$$V_{\text{eff}}(\rho) = \frac{\epsilon^2}{\bar{a}^2} \left( 1 - \frac{2 N_q}{\bar{a}} \rho \right) - \frac{N_q/\bar{a}}{\rho} - \left( \frac{\kappa^2/\bar{a}}{\rho^2} + \frac{\bar{m}_\phi^2}{\bar{a}} \right) \left( 1 - \frac{N_q}{\bar{a}} \rho \right). \quad (78)$$

The metric function  $A(\rho)$ , defined in eq. (77), represents a scenario dominated by string clouds, with a minor perturbation introduced by the presence of quintessence. This interpretation extends to the effective potential (78), which decomposes into terms associated with string clouds and a small quintessence-induced correction. By rearranging the terms in eq. (78) according to powers of  $\rho$ , we obtain:

$$V_{\text{eff}}(\rho) = -\frac{\kappa^2/\bar{a}}{\rho^2} + \left( \frac{\kappa^2}{\bar{a}} - 1 \right) \frac{N_q/\bar{a}}{\rho} + \frac{\epsilon^2 - \bar{a} \bar{m}_\phi^2}{\bar{a}^2} - \left( \epsilon^2 - \frac{1}{2} \bar{a} \bar{m}_\phi^2 \right) \frac{2N_q}{\bar{a}^3} \rho.$$

To solve the differential equation (13) for  $u_{HL}^{(1/2)}(\rho)$  using the effective potential above, we apply the results from eqs. (A.15) and (A.16). This leads to a solution expressed in terms of the confluent Heun function, provided that

$$\epsilon^2 = \frac{1}{2} \bar{a} \bar{m}_\phi^2,$$

which is identical to the constraint of eq. (57) from the standard scenario with  $\alpha_q = 1/2$ . Under this condition, the solution for  $u_{HL}^{(1/2)}(\rho)$  is:

$$u_{HL}^{(1/2)}(\rho) = e^{\alpha\rho/2} \rho^{(1+\beta)/2} (\rho - 1)^{(1+\gamma)/2} [c_1 \text{HeunC}(\alpha, \beta, \gamma, \delta, \eta; \rho) + c_2 \rho^{-\beta} \text{HeunC}(\alpha, -\beta, \gamma, \delta, \eta; \rho)], \quad (79)$$

while the Heun parameters are:

$$\begin{aligned}
\alpha &= \pm \sqrt{\frac{2\bar{m}_\phi^2}{\bar{a}}}, \\
\beta &= \pm \sqrt{1 + \frac{4\kappa^2}{\bar{a}}}, \\
\gamma &= \pm 1, \\
\delta &= \frac{N_q}{\bar{a}} \left( \frac{\kappa^2}{\bar{a}} - 1 \right), \\
\eta &= \frac{1}{2} - \frac{N_q}{\bar{a}} \left( \frac{\kappa^2}{\bar{a}} - 1 \right).
\end{aligned} \tag{80}$$

The radial wave function, determined by eq. (12), is then given by:

$$\begin{aligned}
R_{HL}^{(1/2)}(\rho) &= \left(1 - \frac{N_q}{2\bar{a}}\rho\right) e^{\alpha\rho/2} \rho^{(\beta-1)/2} (\rho-1)^{(1+\gamma)/2} [c_1 \text{HeunC}(\alpha, \beta, \gamma, \delta, \eta; \rho) \\
&\quad + c_2 \rho^{-\beta} \text{HeunC}(\alpha, -\beta, \gamma, \delta, \eta; \rho)].
\end{aligned} \tag{81}$$

From eqs. (77) and (81), we observe that  $R_{HL}^{(1/2)}(0) = 0$  and  $A(0) = \bar{a}$ , confirming the absence of a singularity at  $\rho = 0$ , as expected. For small values of  $\rho$  ( $0 < \rho < 1$ ), the local confluent Heun function can be expressed as:

$$\text{HeunCl}(\alpha, \beta, \gamma, \delta, \eta; \rho) = \sum_{m=0}^{\infty} c_m \rho^m. \tag{82}$$

The coefficients  $c_m$  are determined by the three-term recursion relation specified in eqs. (A.27a)–(A.27d), with  $c_0 = 1$ . Since  $\text{HeunCl}(\alpha, \beta, \gamma, \delta, \eta; \rho) \rightarrow 1$  as  $\rho \rightarrow 0$ , we find that near the origin,  $R_{HL}^{(1/2)}(\rho)$  simplifies to

$$R_{HL}^{(1/2)}(\rho) \approx (\rho-1)^{(1+\gamma)/2} [c_1 \rho^{(\beta-1)/2} + c_2 \rho^{-(\beta+1)/2}]. \tag{83}$$

On the other hand, when there is no quintessence ( $N_q = 0$ ), the effective potential (78) simplifies to

$$V_{\text{eff}}(\rho) = \frac{\epsilon^2 - \bar{a}\bar{m}_\phi^2}{\bar{a}^2} - \frac{\kappa^2/\bar{a}}{\rho^2}, \tag{84}$$

regardless the value of  $\epsilon^2$ . Consequently, if the only matter component in the Universe is the cloud of strings, we use eqs. (12), (13) and (84) to obtain

that the radial wave function for the spin-0 particle becomes

$$R_{HL+F}(\rho) = \rho^{-1/2} \left[ c_1 J_n \left( \sqrt{\frac{\epsilon^2 - \bar{a} \bar{m}_\phi^2}{\bar{a}^2}} \rho \right) + c_2 Y_n \left( \sqrt{\frac{\epsilon^2 - \bar{a} \bar{m}_\phi^2}{\bar{a}^2}} \rho \right) \right], \quad (85)$$

where

$$n = \sqrt{\frac{1}{4} + \frac{\kappa^2}{\bar{a}}}, \quad (86)$$

where  $J_n(\rho)$  and  $Y_n(\rho)$  are the Bessel functions of the first and second kinds, respectively. If we look for solutions near the origin ( $\rho \sim 0$ ), we take  $c_2=0$ . Notably, the result for  $R_{HL+F}(\rho)$  is independent of  $\alpha_q$ , as expected, given the absence of quintessence.

In the restricted scenario where  $\bar{a} \neq 0$ ,  $\rho_s = 0$ ,  $N_q = 0$ , and  $\epsilon^2 = \bar{a} \bar{m}_\phi^2$ , the effective potential in eq. (84) simplifies to a single term proportional to  $\rho^{-2}$ . Under these conditions, eq. (13) reduces to a Cauchy-Euler equation. Solving this equation for  $u_{HL+F}^\diamond(\rho)$  and employing eq. (12), we obtain the radial wave function:

$$R_{HL+F}^\diamond(\rho) = c_1 \rho^{-1/2+n} + c_2 \rho^{-1/2-n}, \quad (87)$$

where  $n \in \mathbb{R}$  is defined by eq. (86) and satisfies  $n \geq 1/2$ . This ensures the radial wave function satisfies  $R_{HL+F}^\diamond(0) = 0$  only if  $c_2 = 0$ . The symbol  $\diamond$  denotes the special case of the radial wave function characterized by the defined spectrum  $\epsilon^2 = \bar{a} \bar{m}_\phi^2$ . Therefore, to describe the wave function near the origin, we consider  $c_2 = 0$ . For large  $\rho$ , we set  $c_1 = 0$  to prevent a divergent wave function.

Having derived the radial wave functions in eqs. (61), (69), (76), (81), (85) and (87) for the specific case of  $\alpha_q = 1/2$  and established their validity over a broad range of radial coordinates, we now proceed to investigate the upper bound of  $\alpha_q = 1$  in the following section. The comprehensive set of wave functions obtained in this analysis will provide valuable insights into the behavior of solutions for other values of  $\alpha_q$ .

## 5. Solutions for the upper bound

This section explores solutions to the radial Klein-Gordon equation when  $\alpha_q = 1$ , which corresponds to the limiting case of  $\omega_q = -1$ . We investigate the behavior of these solutions in three distinct scenarios: the standard case (including black strings, string clouds, and quintessence), the cloudless case

(excluding string clouds), and the horizonless case (without the black string). For each scenario, we derive the radial wave function of the scalar particle using Bessel and Heun equations, providing a detailed analysis of particle dynamics within this regime.

To solve the radial Klein-Gordon equation (10) using eqs. (12)–(14) with  $\alpha_q = 1$ , we first rewrite  $A(\rho)$ , given by eq. (8), in terms of the dimensionless variable  $x$ , to show that

$$A(\rho) = \bar{a} - \frac{\rho_s}{\rho_+} \frac{1}{x} + N_{qL} \rho_+^2 x^2, \quad (88)$$

where

$$N_{qL} = N_q + 1/l^2. \quad (89)$$

In this regime, the contributions from quintessence and the cosmological constant combine (they both depend on  $\rho^2$ ); therefore, we need not approximate the term  $\rho^2/l^2$  in eq. (8). Consequently, the solutions we will discuss in this regime are exact for all values of the radial coordinate.

As shown in our previous work [36], when  $\alpha_q = 1$ , with  $\bar{a} \neq 0$ ,  $\rho_s \neq 0$ , and  $N_{qL} \neq 0$ , the event horizon  $\rho_+$  is given by

$$\rho_+ = \Delta^{1/3} - \frac{\bar{a}}{3N_{qL}} \Delta^{-1/3}, \quad (90)$$

with

$$\Delta = \left( \frac{\bar{a}}{3N_{qL}} \right)^{3/2} \left[ \left( 1 + \frac{27 N_{qL} \rho_s^2}{4 \bar{a}^3} \right)^{1/2} + \left( \frac{27 N_{qL} \rho_s^2}{4 \bar{a}^3} \right)^{1/2} \right].$$

Considering the scenario where  $N_{qL} \rho_s^2 / \bar{a}^3 \ll 1$ , given that  $N_{qL} \sim 10^{-52} \text{ m}^{-2}$ , the event horizon of eq. (90) simplifies to

$$\rho_+ = \frac{\rho_s}{\bar{a}},$$

to first order in  $N_{qL} \rho_s^2 / \bar{a}^3$ , implying that

$$N_{qL} \rho_+^2 = \frac{N_{qL} \rho_s^2}{\bar{a}^2}.$$

Substituting the above result into eq. (88), we obtain

$$A(x) = \bar{a} \left( 1 - \frac{1}{x} + \frac{N_{qL} \rho_s^2}{\bar{a}^3} x^2 \right). \quad (91)$$

The result of eq. (91) can be seen as a first-order correction to the case where quintessence is absent, given by eq. (42). Recalling that the cloud parameter  $\bar{a}$  would typically range from  $10^{-6}$  to  $10^1$ , with  $\rho_s$  ranging from  $10^{-2}$  to  $10^{15}$  m, the term  $N_{ql} \rho_s^2 / \bar{a}^3$  takes values in the interval  $(10^{-60}, 10^{-4})$ , which satisfies our constraint

$$\frac{N_{ql} \rho_s^2}{\bar{a}^3} \ll 1. \quad (92)$$

In principle, we could search for analytic solutions of the radial wave function  $R_{ST}^{(1)}(x)$  with  $A(x)$  being in the form of eq. (91). However, the resulting differential equation for the auxiliary function  $u_{ST}^{(1)}(x)$  does not present simple analytic solutions, even when we explore special cases with additional constraints on  $\epsilon$  and  $\bar{m}_\phi$ . Therefore, we solve the problem by dividing it into two distinct regions: one near the event horizon, where  $x \rightarrow 1^+$ , and the other for larger values of  $x$ .

### 5.1. Near the event horizon

The solution near the event horizon, when  $x \rightarrow 1^+$ , is given by eqs. (20) and (21), where the factor  $\beta_+$ , defined by eq. (19), becomes

$$\beta_+ = \bar{a} \left( 1 + \frac{2N_{ql} \rho_s^2}{\bar{a}^3} \right).$$

This result is obtained by substituting the simplified event horizon expression,  $\rho_+ = \rho_s / \bar{a}$  (please, see table 2), which is valid under the approximation  $N_{ql} \rho_s^2 / \bar{a}^3 \ll 1$ , into the general expression for  $\beta_+$ .

Therefore, when  $x \rightarrow 1^+$ , the radial wave function behaves according to eq. (22), implying

$$\begin{aligned} R_{ST}^{(1)}(x) = & c_1 \exp \left[ \frac{\gamma}{2} \ln(x-1) + \frac{\beta}{2}(x-1) \right] \\ & + c_2 \exp \left[ \frac{\gamma}{2} \ln(x-1) - \frac{\beta}{2}(x-1) \right], \end{aligned} \quad (93)$$

where the Heun parameters  $\gamma$  and  $\beta$  are determined by eq. (21) and, in this case, are explicitly given by

$$\begin{aligned} \frac{\gamma}{2} = & i\epsilon \frac{\rho_s}{\bar{a}^2} \left( 1 - \frac{2N_{ql} \rho_s^2}{\bar{a}^3} \right), \\ \frac{\beta}{2} = & \left( \frac{1}{4} - \frac{\kappa^2}{\bar{a}} \right)^{1/2} + \left( \frac{1}{4} - \frac{\kappa^2}{\bar{a}} \right)^{-1/2} \frac{\kappa^2}{\bar{a}} \frac{N_{ql} \rho_s^2}{\bar{a}^3}, \end{aligned} \quad (94)$$

where we used the constraint of eq. (92). The phase shift caused by the presence of dark energy, which we termed the *dark phase*, shall be discussed in details at section 6.

### 5.2. Far from the event horizon

For larger values of  $x$ , away from the event horizon (at  $x = 1$ ), we can simplify the expression of eq. (91) to determine the radial wave function in this regime. As  $x$  increases, the term  $1/x$  decreases, implying we can approximate  $A(x)$  as

$$A(x) = \bar{a} \left( 1 + \frac{N_{ql} \rho_s^2}{\bar{a}^3} x^2 \right). \quad (95)$$

In fig. 1, we show a comparison between the exact expression of eq. (91), the approximation of eq. (95), and the case without quintessence given by eq. (42), where we chose  $N_{ql} \rho_s^2 / \bar{a}^3 = 6.2 \times 10^{-5}$  and the variable  $x$  taking values in the interval  $[1, 100]$ . Notably, as  $N_{ql} \rho_s^2 / \bar{a}^3$  decreases, larger values of  $x$  are required to observe a noticeable difference between the approximation of eq. (95) and the exact solution of eq. (91).

The effective potential  $\rho_+^2 V_{\text{eff}}(x)$ , defined by eq. (17), following from the expression (95), takes the form of

$$\begin{aligned} \rho_+^2 V_{\text{eff}}(x) &= \left( \frac{\epsilon \rho_s}{\bar{a}^2} \right)^2 \left( 1 - \frac{2N_{ql} \rho_s^2}{\bar{a}^3} x^2 \right) \\ &\quad - \frac{3N_{ql} \rho_s^2}{\bar{a}^3} - \left( \frac{\kappa^2 / \bar{a}}{x^2} + \frac{\rho_s^2 \bar{m}_\phi^2}{\bar{a}^3} \right) \left( 1 - \frac{N_{ql} \rho_s^2}{\bar{a}^3} x^2 \right). \end{aligned}$$

We can rearrange the above expression in terms of powers of  $x$  to see that

$$\begin{aligned} \rho_+^2 V_{\text{eff}}(x) &= -\frac{\kappa^2 / \bar{a}}{x^2} + \frac{\rho_s^2}{\bar{a}^4} \left[ (\epsilon^2 - \bar{a} \bar{m}_\phi^2) - N_{ql} (3\bar{a} - \kappa^2) \right] \\ &\quad - \left( 2\epsilon^2 - \bar{a} \bar{m}_\phi^2 \right) \frac{N_{ql} \rho_s^4}{\bar{a}^7} x^2. \end{aligned} \quad (96)$$

The solution to eq. (16) with a potential in the form of (96) is expressed in terms of the Biconfluent Heun function,  $\text{HeunB}(\alpha, \beta, \gamma, \delta; x)$ , as defined by eqs. (B.3) and (B.4). Therefore, we can use a change of variables to put the equation for  $u_{st}^{(1)}(x)$  into the form of eq. (B.3). To do so, we define

$$z = (2Q)^{1/4} x, \quad (97)$$

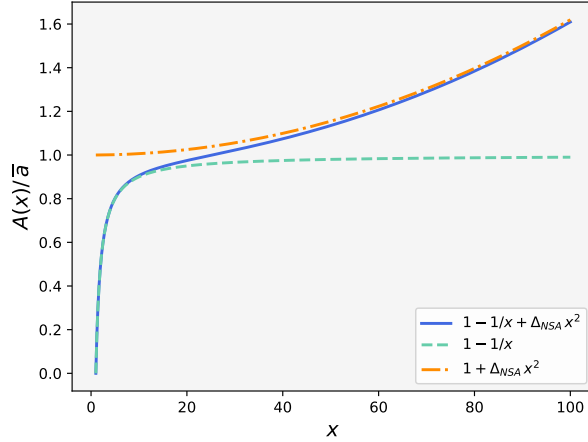


Figure 1: Comparison of  $A(x)/\bar{a}$  for  $x \in [1, 100]$ , with a fixed value of  $\Delta_{NSA} = N_{QL} \rho_S^2 / \bar{a}^3 = 6.2 \times 10^{-5}$ . The solid line shows the exact case of eq. (91), the dashed line represents the case without quintessence, and the dash-dotted line neglects the  $1/x$  term. This comparison highlights the impact of quintessence and the  $1/x$  term on the behavior of  $A(x)/\bar{a}$ . We stress that, as the value of  $N_{QL} \rho_S^2 / \bar{a}^3$  decreases, it becomes more difficult to distinguish these lines.

with

$$Q = \left(2\epsilon^2 - \bar{a} \bar{m}_\phi^2\right) \frac{N_{QL} \rho_S^4}{\bar{a}^7}. \quad (98)$$

The derivative in  $x$  is related to the derivative in  $z$  so that

$$\frac{d^2}{dx^2} = (2Q)^{1/2} \frac{d^2}{dz^2},$$

then, eq. (16) becomes

$$\frac{d^2}{dz^2} u_{ST}^{(1)} + \frac{\rho_+^2 V_{\text{eff}}(z)}{(2Q)^{1/2}} u_{ST}^{(1)}(z) = 0, \quad (99)$$

where  $\rho_+^2 V_{\text{eff}}(z)$  comes from eq. (96) so that

$$\frac{\rho_+^2 V_{\text{eff}}(z)}{(2Q)^{1/2}} = -\frac{1}{2} z^2 + \frac{1}{(2\bar{a}N_{QL})^{1/2}} \frac{(\epsilon^2 - \bar{a} \bar{m}_\phi^2) - \bar{a}N_{QL}(3 - \kappa^2/\bar{a})}{(2\epsilon^2 - \bar{a} \bar{m}_\phi^2)^{1/2}} - \frac{\kappa^2/\bar{a}}{z^2}, \quad (100)$$

as long as  $(2\epsilon^2 - \bar{a}\bar{m}_\phi^2) \neq 0$ , which ensures that  $Q$  is non-zero, allowing for the change of variables. Therefore, the solution to  $u_{ST}^{(1)}(z)$  is

$$u_{ST}^{(1)}(z) = u_0 z^{(1+\alpha)/2} e^{-\beta z/2} e^{-z^2/2} \text{HeunB}(\alpha, \beta, \gamma, \delta; z),$$

with

$$\begin{aligned} \alpha &= \pm \sqrt{1 + \frac{4\kappa^2}{\bar{a}}}, \\ \beta &= 0, \\ \gamma &= \frac{1}{(2\bar{a}N_{ql})^{1/2}} \frac{(\epsilon^2 - \bar{a}\bar{m}_\phi^2) - \bar{a}N_{ql}(3 - \kappa^2/\bar{a})}{(2\epsilon^2 - \bar{a}\bar{m}_\phi^2)^{1/2}}, \\ \delta &= 0. \end{aligned} \tag{101}$$

As a consequence, the radial wave function associated with  $\alpha_q = 1$  with  $\bar{a} \neq 0$ ,  $\rho_s \neq 0$ , and  $N_{ql} \neq 0$ , for  $x \gg 1$ , is given by

$$R_{ST}^{(1)}(z) = R_0 \left[ 1 - \frac{N_{ql}\rho_s^2}{2\bar{a}^3} \frac{z^2}{(2Q)^{1/2}} \right] z^{(-1+\alpha)/2} e^{-z^2/2} \text{HeunB}(\alpha, \beta, \gamma, \delta; z), \tag{102}$$

provided that  $(2\epsilon^2 - \bar{a}\bar{m}_\phi^2) \neq 0$ . Here,  $Q$  is defined by eq. (98),  $z$  by eq. (97), while the parameters of the Biconfluent Heun function are given by eq. (101). The pre-factor, to the right of the normalization constant  $R_0$ , arises from the first order approximation of  $A(x)^{-1/2}$ , occurring at eq. (12), at large  $x$  values. It is interesting to note that when the spin-0 particle is far from the event horizon, it behaves as if there were no horizon at all.

If we apply the condition (B.8) to require that  $\text{HeunB}(\alpha, \beta, \gamma, \delta; z)$  is truncated into a  $N$ -th order polynomial, we obtain a constraint on the energy  $\epsilon$ , given by:

$$\frac{1}{(2\bar{a}N_{ql})^{1/2}} \frac{(\epsilon^2 - \bar{a}\bar{m}_\phi^2) - \bar{a}N_{ql}(3 - \kappa^2/\bar{a})}{(2\epsilon^2 - \bar{a}\bar{m}_\phi^2)^{1/2}} \mp \left(1 + \frac{4\kappa^2}{\bar{a}}\right)^{1/2} = 2N + 2, \tag{103}$$

with  $N \in \mathbb{Z}^+$ . It is important to remember that the above constraint provides only those energy eigenvalues associated with polynomial solutions. If, for instance,  $\epsilon^2 = \bar{a}\bar{m}_\phi^2$ , then eq. (103) simplifies to

$$\left(\frac{N_{ql}}{8\bar{m}_\phi^2}\right)^{1/2} \left(\frac{\kappa^2}{\bar{a}} - 3\right) \mp \left(\frac{1}{4} + \frac{\kappa^2}{\bar{a}}\right)^{1/2} = N + 1, \tag{104}$$

which is a lot simpler than (103). Of course, other relations between  $\epsilon^2$  and  $\bar{a} \bar{m}_\phi^2$  are possible, provided  $2\epsilon^2 \neq \bar{a} \bar{m}_\phi^2$ .

On the other hand, when  $\epsilon^2$  satisfies  $2\epsilon^2 = \bar{a} \bar{m}_\phi^2$ , there is a simpler solution to this problem since the effective potential (96) simplifies to

$$\rho_+^2 V_{\text{eff}}(x) = -\frac{\kappa^2/\bar{a}}{x^2} - V_0, \quad (105)$$

where

$$V_0 = \frac{\rho_s^2}{2\bar{a}^3} \left[ \bar{m}_\phi^2 + 2N_{ql} \left( 3 - \kappa^2/\bar{a} \right) \right].$$

Therefore, solving the equation for  $u_{ST}^{(1,\odot)}(x)$  with the simpler effective potential of eq. (105), we obtain that

$$u_{ST}^{(1,\odot)}(x) = \sqrt{x} \left[ c_1 I_n \left( \sqrt{V_0} x \right) + c_2 K_n \left( \sqrt{V_0} x \right) \right],$$

where  $I_n(x)$  and  $K_n(x)$  are the modified Bessel functions of the first and second kinds, respectively. The order  $n$  is given by  $n = \sqrt{1/4 + \kappa^2/\bar{a}}$ , just like the case of eq. (86).

Note that the symbol “ $\odot$ ” was included as a label to distinguish this particular case, of  $2\epsilon^2 = \bar{a} \bar{m}_\phi^2$ , from the general result given by eq. (102). From the above result for  $u_{ST}^{(1,\odot)}(x)$ , we can determine the associated radial wave function using eq. (12), to show that

$$R_{ST}^{(1,\odot)}(x) = x^{-1/2} \left( 1 - \frac{N_{ql} \rho_s^2}{2\bar{a}^2} x^2 \right) \left[ c_1 I_n \left( \sqrt{V_0} x \right) + c_2 K_n \left( \sqrt{V_0} x \right) \right], \quad (106)$$

where, again, we have used a first-order approximation of  $A(x)^{-1/2}$ , used in eq. (95), in accordance with the regime where  $N_{ql} \rho_s^2/\bar{a}^3 \ll 1$ . However, there is a final consideration due to the fact that solution (106) is valid for all  $x \gg 1$ , and it is unbounded. To obtain the desired behavior of the radial wave function as  $x$  approaches infinity, we set  $c_1 = 0$  because only  $K_n(x)$  is a decreasing function of  $x$ . Therefore:

$$R_{ST}^{(1,\odot)}(x) = \frac{R_0}{\sqrt{x}} \left( 1 - \frac{N_{ql} \rho_s^2}{2\bar{a}^2} x^2 \right) K_n \left( \sqrt{V_0} x \right), \quad (107)$$

where  $R_0$  is a normalization constant and  $n$  is defined by eq. (86).

### 5.3. Cloudless at the upper bound

In the preceding analysis, we solved the limiting case of  $\alpha_q = 1$ , where  $\bar{a} \neq 0$ ,  $\rho_s \neq 0$ , and  $N_{ql} \neq 0$ . However, solutions (102) and (106) do not hold if  $\bar{a} = 0$ . To solve the problem for this cloudless scenario, let us consider the general result for  $A(\rho)$ , given by eq. (8), as we set  $\bar{a} = 0$  and use the definition of  $N_{ql}$  from eq. (89) to obtain that

$$A(\rho) = N_{ql} \rho^2 - \frac{\rho_s}{\rho}.$$

After requiring that  $A(\rho_+) = 0$ , we conclude that  $\rho_+ = (\rho_s/N_{ql})^{1/3}$ , implying we can write the above result in terms of the dimensionless variable  $x$ , resulting in

$$A(x) = \left(N_{ql} \rho_s^2\right)^{1/3} \left(x^2 - \frac{1}{x}\right). \quad (108)$$

Notably, this result for  $A(x)$  is valid for all  $x > 1$ , that is, the whole domain of the radial coordinate.

As  $x \rightarrow 1^+$ , we recover the conditions of the solution (20), with  $\beta_+$ , defined by eq. (19), being  $\beta_+ = 3(N_{ql} \rho_s^2)^{1/3}$ . Therefore, near the event horizon, the spin-0 particle's wave function is given by eq. (22) with the Heun parameters  $\gamma$  and  $\beta$ , defined by (21), which are explicitly:

$$\begin{aligned} \frac{\gamma}{2} &= \pm \frac{i\epsilon}{\left(27N_{ql}^2 \rho_s\right)^{1/3}}, \\ \frac{\beta}{2} &= \pm \left[ \frac{1}{4} - \frac{\kappa^2}{3(N_{ql} \rho_s^2)^{1/3}} \right]^{1/2}. \end{aligned} \quad (109)$$

Similar to the parameters from eq. (94), the above expressions for  $\gamma$  and  $\beta$  will also have implications in terms of dark phases, but we leave this discussion to section 6.

Next, we investigate the solution for  $x > 1$ , where it is a good approximation of eq. (108) to consider

$$A(x) = \left(N_{ql} \rho_s^2\right)^{1/3} x^2. \quad (110)$$

This approximation is good for values of  $x$  away from the event horizon and improves as  $x$  increases. The approximation is valid as long as  $x > 1$ , but it

is reasonable to take  $x > 5$ , for instance, so that the relative error in  $A(x)$  is less than 1%.

Using the effective potential (17) with  $A(x)$  approximated by (110), gives

$$\rho_+^2 V_{\text{eff}}(x) = - \left( 2 + \frac{\bar{m}_\phi^2}{N_{QL}} \right) \frac{1}{x^2} + \left[ \frac{\epsilon^2}{(N_{QL}^2 \rho_S)^{2/3}} - \frac{\kappa^2}{(N_{QL} \rho_S^2)^{1/3}} \right] \frac{1}{x^4}. \quad (111)$$

Thus, the general solution for  $u_{CL}^{(1)}(x)$  is given by:

$$u_{CL}^{(1)}(x) = x^{1/2} \left[ c_1 J_\ell \left( \frac{\sqrt{m}}{x} \right) + c_2 Y_\ell \left( \frac{\sqrt{m}}{x} \right) \right], \quad (112)$$

where

$$\ell = \sqrt{\frac{9}{4} + \frac{\bar{m}_\phi^2}{N_{QL}}}, \quad (113)$$

$$m = \frac{\epsilon^2}{(N_{QL}^2 \rho_S)^{2/3}} - \frac{\kappa^2}{(N_{QL} \rho_S^2)^{1/3}}.$$

It follows from eqs. (12) and (112) that

$$R_{CL}^{(1)}(x) = x^{-3/2} \left[ c_1 J_\ell \left( \frac{\sqrt{m}}{x} \right) + c_2 Y_\ell \left( \frac{\sqrt{m}}{x} \right) \right], \quad (114)$$

where  $\ell$  and  $m$  are defined by (113) and the constants  $c_1$  and  $c_2$  absorbed the remaining multiplicative factors. If we are interested in the region of large  $x$ , i.e.,  $x \gg 1$ , we must set  $c_2 = 0$  to prevent the radial wave function from diverging.

Conversely, if  $m$ , defined by eq. (113), is set to  $m = 0$ , implying the restricted case where

$$\epsilon^2 = \kappa^2 N_{QL}, \quad (115)$$

the effective potential (111), valid for  $x > 1$ , simplifies to

$$\rho_+^2 V_{\text{eff}}(x) = - \left( 2 + \frac{\bar{m}_\phi^2}{N_{QL}} \right) \frac{1}{x^2},$$

implying eq. (16), for  $u_{CL}^{(1, \boxtimes)}(x)$ , is a Cauchy-Euler equation of the form

$$u_{CL}^{(1, \boxtimes)}(x) = c_1 x^{1/2+\ell} + c_2 x^{1/2-\ell},$$

where  $\ell$  is given by eq. (113) and the symbol “ $\boxtimes$ ” is used only to distinguish this particular case, satisfying eq. (115), from the general solution of eq. (114). Using eq. (12), we obtain that the radial wave function  $R_{CL}^{(1,\boxtimes)}(x)$  is given by

$$R_{CL}^{(1,\boxtimes)}(x) = c_1 x^{-3/2+\ell} + c_2 x^{-3/2-\ell},$$

where – again –  $c_1$  and  $c_2$  absorbed multiplicative constants. Since the domain is unbounded ( $x > 1$ ), we require that  $c_1 = 0$  because  $\ell > 3/2$ , implying

$$R_{CL}^{(1,\boxtimes)}(x) = R_0 x^{-3/2-\ell},$$

where we renamed  $c_2$  to  $R_0$  as the remaining normalization constant.

#### 5.4. Horizonless at the upper bound

In this final case, we remove the black string contribution setting  $\rho_s = 0$ , but we keep the clouds of strings ( $\bar{a} \neq 0$ ), and the quintessence fluid (with  $\alpha_q = 1$ ). Once more, since  $N_{ql}$ , defined by eq. (89), takes into account the role of  $l^{-2}$ , we do not need to restrict the range of  $\rho$ . This scenario simplifies eq. (8), describing the general  $A(\rho)$  as

$$A(\rho) = \bar{a} \left( 1 + \frac{N_{ql}}{\bar{a}} \rho^2 \right), \quad (116)$$

where  $N_{ql}/\bar{a}$  would typically range from  $10^{-52} \text{ m}^{-2}$  to  $10^{-46} \text{ m}^{-2}$ , implying its contribution is negligible unless  $\rho \gg 1$ , specifically of the order of  $\rho_{obs.} \sim |l|$ . Notably, eq. (116) describing  $A(\rho)$  is very similar to eq. (95), but with a difference in the domain because this case without an event horizon starts at  $\rho = 0$  and cannot be written in terms of the dimensionless variable  $x$ . The result from eq. (116) can also be interpreted as a tiny correction to the case without quintessence, where only  $\bar{a}$  is nonzero.

From eq. (116), we obtain the effective potential  $V_{\text{eff}}(\rho)$ , defined by eq. (14), as

$$V_{\text{eff}}(\rho) = \frac{\epsilon^2}{\bar{a}^2} \left( 1 - \frac{2 N_{ql}}{\bar{a}} \rho^2 \right) - \frac{3 N_{ql}}{\bar{a}} - \left( \frac{\kappa^2/\bar{a}}{\rho^2} + \frac{\bar{m}_\phi^2}{\bar{a}} \right) \left( 1 - \frac{N_{ql}}{\bar{a}} \rho^2 \right), \quad (117)$$

where we have neglected quadratic and higher order terms in  $N_{ql}$ . Note that the result above is very similar to the case of eq. (78), where  $\alpha_q$  was in the middle of its interval. This similarity follows from the fact that, in both cases, quintessence is just a tiny correction to the respective  $A(\rho)$ .

To investigate the solution associated with the effective potential (117), we rewrite it more conveniently:

$$V_{\text{eff}}(\rho) = - \left( \frac{2\epsilon^2 - \bar{a} \bar{m}_\phi^2}{\bar{a}^2} \right) \frac{N_{qL}}{\bar{a}} \rho^2 + \left( \frac{\epsilon^2 - \bar{a} \bar{m}_\phi^2}{\bar{a}^2} \right) - \frac{\kappa^2/\bar{a}}{\rho^2}. \quad (118)$$

We recall that the terms  $3N_{qL}/\bar{a}$  and  $\kappa^2 N_{qL}/\bar{a}^2$  were excluded due to their negligible contribution.

After joining eq. (13) for  $u_{HL}^{(1)}(\rho)$  with the potential (118), we see that our problem is almost in the form of a Biconfluent Heun equation such as eq. (B.3). Thus, we can change variables from  $\rho$  to  $z = (2P)^{1/4} \rho$ , analogous to eq. (97), where now

$$P = \left( \frac{2\epsilon^2 - \bar{a} \bar{m}_\phi^2}{\bar{a}^3} \right) N_{qL}, \quad (119)$$

provided  $2\epsilon^2 - \bar{a} \bar{m}_\phi^2 \neq 0$ . Under this change of variables, we use the result of eq. (99) simply replacing ‘‘Q’’ with a ‘‘P’’ to determine the term corresponding to  $V_{\text{eff}}(z)$ :

$$\frac{V_{\text{eff}}(z)}{(2P)^{1/2}} = -\frac{1}{2} z^2 + \frac{1}{\sqrt{2\bar{a}}} \frac{\epsilon^2 - \bar{a} \bar{m}_\phi^2}{(2\epsilon^2 - \bar{a} \bar{m}_\phi^2)^{1/2}} - \frac{\kappa^2/\bar{a}}{z^2}. \quad (120)$$

Therefore, comparing eqs. (99) and (120) with the general result (B.1), we conclude that  $u_{HL}^{(1)}(z)$  is

$$u_{HL}^{(1)}(z) = u_0 z^{(1+\alpha)/2} e^{-z^2/2} \text{HeunB}(\alpha, \beta, \gamma, \delta; z),$$

with

$$\begin{aligned} \alpha &= \pm \sqrt{1 + \frac{4\kappa^2}{\bar{a}}}, \\ \beta &= 0, \\ \gamma &= \frac{1}{\sqrt{2\bar{a}}} \frac{\epsilon^2 - \bar{a} \bar{m}_\phi^2}{(2\epsilon^2 - \bar{a} \bar{m}_\phi^2)^{1/2}}, \\ \delta &= 0. \end{aligned} \quad (121)$$

As a consequence, the radial wave function associated with  $\alpha_q = 1$  with  $\rho_s = 0$  is given by

$$R_{HL}^{(1)}(z) = \frac{R_0}{z} \left[ 1 - \frac{N_{qL}}{2\bar{a}} \frac{z^2}{(2P)^{1/2}} \right] z^{(1+\alpha)/2} e^{-z^2/2} \text{HeunB}(\alpha, \beta, \gamma, \delta; z), \quad (122)$$

where  $P$  is given by eq. (119),  $z$  by eq. (97), while the parameters of the Biconfluent Heun function are determined by eq. (121).

Applying the condition of eq. (B.8) to require that  $\text{HeunB}(\alpha, \beta, \gamma, \delta; z)$  becomes an  $N$ -th order polynomial, we find that:

$$\frac{1}{\sqrt{2}\bar{a}} \frac{\epsilon^2 - \bar{a}\bar{m}_\phi^2}{(2\epsilon^2 - \bar{a}\bar{m}_\phi^2)^{1/2}} \mp \left(1 + \frac{4\kappa^2}{\bar{a}}\right)^{1/2} = 2N + 2, \quad (123)$$

with  $N \in \mathbb{Z}^+$ . The above constraint provides only those energy eigenvalues associated with polynomial solutions. For example, if  $\epsilon^2 = \bar{a}\bar{m}_\phi^2$ , then eq. (123) simplifies to

$$\left(1 + \frac{4\kappa^2}{\bar{a}}\right)^{1/2} = 2N + 2,$$

which implies that the spin-0 particle's momentum along the  $z$ -coordinate is quantized, with the allowed values determined by the order of the Heun polynomial.

It is interesting to note that, when

$$\epsilon^2 = \bar{a}\bar{m}_\phi^2,$$

the effective potential (117) reduces to

$$V_{\text{eff}}(\rho) = -\frac{\bar{m}_\phi^2}{\bar{a}^2} N_{\text{ql}} \rho^2 - \frac{\kappa^2/\bar{a}}{\rho^2}. \quad (124)$$

The formal solution to  $u_{HL}^{(1,\triangleright)}$  can also be written in terms of the modified Bessel functions. However, since  $N_{\text{ql}}/\bar{a}^2$  ranges from  $10^{-54} \text{ m}^{-2}$  to  $10^{-40} \text{ m}^{-2}$ , unless  $\rho$  is huge, of the order of  $10^{20} \text{ m}$  or larger, the dominant contribution for the above effective potential comes from  $-(\kappa^2/\bar{a})/\rho^2$ . Using eqs. (12) and (13), we obtain:

$$R_{HL}^{(1,\triangleright)}(\rho) = c_1 \rho^{-1/2+n} + c_2 \rho^{-1/2-n},$$

where  $n$  is defined by eq. (86) so that  $n \geq 1/2$ . Moreover, we used that  $A(\rho)^{-1} \approx \bar{a}^{-1/2}$  in the regime described above. As in the previous analysis, we use the symbol “ $\triangleright$ ” to distinguish this special case from the general one. We set  $c_2 = 0$  for particles near the origin to avoid a divergence. For large  $\rho$ , we choose  $c_1 = 0$  to prevent  $R_{HL}^{(1,\triangleright)}(\rho) \rightarrow \infty$ .

At very large distances, when  $\rho \gg \sqrt{\kappa^2/(\bar{m}_\phi^2 N_{QL})}$ , the term proportional to  $\rho^2$  dominates the potential (124), which approximates that of a harmonic oscillator, provided  $\bar{m}_\phi \neq 0$ . In this regime, using eqs. (12) and (13), we see that the radial wave function becomes

$$R_{HL}^{(1,\triangleright)}(\rho \gg 1) = \frac{R_0}{\rho} \frac{\sin\left(\frac{\bar{m}_\phi}{a} N_{QL}^{1/2} \rho + \delta_0\right)}{\left(1 + \frac{N_{QL}}{a} \rho^2\right)^{1/2}}, \quad (125)$$

where  $\delta_0$  is an arbitrary phase constant, and  $R_0$  is a normalization constant. The factor  $(1 + N_{QL} \rho^2/a)^{-1/2}$  arises from the approximation of  $A(\rho)^{-1/2}$ .

As our last investigation, we consider the special case when

$$\epsilon^2 = \frac{1}{2} \bar{a} \bar{m}_\phi^2,$$

which is the same constraint as eq. (57), implying that the potential (118) simplifies to

$$V_{\text{eff}}(\rho) = -\frac{\bar{m}_\phi^2}{2\bar{a}} - \frac{\kappa^2/\bar{a}}{\rho^2}. \quad (126)$$

In this case, the solution for  $u_{HL}^{(1,\otimes)}(\rho)$ , associated with eqs. (13) and (126), is in the form of

$$u_{HL}^{(1,\otimes)}(\rho) = \sqrt{\rho} \left[ c_1 I_n \left( \sqrt{\frac{\bar{m}_\phi^2}{2\bar{a}}} \rho \right) + c_2 K_n \left( \sqrt{\frac{\bar{m}_\phi^2}{2\bar{a}}} \rho \right) \right],$$

where again  $I_n(\rho)$  and  $K_n(\rho)$  are the modified Bessel functions of the first and second kinds, respectively,  $n$  is defined by eq. (86), and the “ $\otimes$ ” symbol is used to avoid ambiguities with the general case. From the relation (12), and the first-order approximation to  $A(\rho)$  (with respect to  $N_{QL}/\bar{a}$ ), we conclude that the radial function in this regime is given by:

$$R_{HL}^{(1,\otimes)}(\rho) = \rho^{-1/2} \left( 1 - \frac{N_{QL}}{2\bar{a}} \rho^2 \right) \left[ c_1 I_n \left( \sqrt{\frac{\bar{m}_\phi^2}{2\bar{a}}} \rho \right) + c_2 K_n \left( \sqrt{\frac{\bar{m}_\phi^2}{2\bar{a}}} \rho \right) \right]. \quad (127)$$

To describe particles near the origin, we set  $c_2 = 0$  for appropriate behavior. However, for large values of  $x$ , the radial function must have  $c_1 = 0$  so that it is monotonically decreasing.

## 6. Dark phases for extended solutions

Our preceding analyses have explored solutions to the Klein-Gordon equation across various scenarios, including the standard, cloudless, and horizonless cases. For quintessence parameters  $\alpha_q = 0$  or  $1/2$ , these solutions are valid within a large domain of the radial coordinate, provided  $\rho$  and  $\rho_+$  are significantly smaller than the AdS radius  $l$ . Conversely, when  $\alpha_q = 1$ , our domain is unrestricted, owing to  $N_{ql}$  incorporating the combined contributions of quintessence and the cosmological constant. Any further approximations and/or constraints were chosen to describe the particle’s wave function for specific regimes.

In this section, we explore the implications of our preceding results. Specifically, we investigate cases where the radial wave function, associated with eq. (9), can be expressed as a product of two functions: one independent of the quintessence parameter  $N_q$ , and the other exhibiting explicit dependence on  $N_q$ , usually in the form of a phase difference.

In a previous work [36], we had defined this quintessence-induced phase difference as a “dark phase” and presented a general procedure for determining these possible quantum observables using the Heun parameters  $\gamma$  and  $\beta$ , which are functions of  $\rho_+$  and  $\beta_+$ . This result was related to the solution of eqs. (12) and (13) under a first-order approximation of the metric function  $A(x) = \beta_+(x - 1)$ , valid near the horizon ( $x \rightarrow 1^+$ ), leading to the solution of eq. (22). Although this was a general result, it could not handle scenarios without an event horizon and could not account for higher-order corrections to these dark phases if the spin-0 particle was distant from the horizon.

However, our novel extended solutions overcome these limitations. We further demonstrate that, in specific cases, the dependence on  $N_q$  can be factored straightforwardly, enabling the determination of dark phases. Moreover, we will explore dark phases in horizonless scenarios and provide examples within standard and cloudless regimes.

### 6.1. Dark phases for the lower bound

To examine the influence of quintessence on the radial wave function when  $\alpha_q = 0$ , we analyze the behavior of eq. (31) as  $x \rightarrow 1^+$ . This yields the following approximation:

$$R_{ST}^{(0)}(x) = R_0 \exp \left[ \frac{\gamma}{2} \ln(x - 1) + \frac{\alpha}{2} \right]. \quad (128)$$

Higher-order approximations, within the domain of validity of the Frobenius solution given by eq. (A.34), would introduce corrections to the coefficient of  $\ln(x-1)$ . In contrast, due to  $\exp(\alpha x/2)$  we would have corrections to powers of  $(x-1)$ . However, the logarithmic term dominates the radial wave function as  $x$  approaches  $1^+$  (the event horizon). Consequently, we can use the above approximation as a fundamental term for analyzing higher-order cases. The Heun parameters for the standard scenario with  $\alpha_q = 0$ , given by eq. (30), can be expressed as:

$$\begin{aligned}\frac{\gamma}{2} &= \pm i \frac{\epsilon \rho_s}{(\bar{a} + N_q)^2}, \\ \frac{\alpha}{2} &= \pm i \frac{\rho_s}{(\bar{a} + N_q)^2} \sqrt{\epsilon^2 - (\bar{a} + N_q) \bar{m}_\phi^2}.\end{aligned}\tag{129}$$

Substituting the expressions for the Heun parameters  $\gamma$  and  $\alpha$ , as defined in eq. (129), into the radial wave function (128), we arrive at:

$$R_{st}^{(0)}(x) = R_0 \exp \left\{ \pm i \frac{\rho_s}{(\bar{a} + N_q)^2} \left[ \epsilon \ln(x-1) + \sqrt{\epsilon^2 - (\bar{a} + N_q) \bar{m}_\phi^2} \right] \right\},\tag{130}$$

where the expression inside the brackets may be interpreted as an implicit dark phase for this case. The real part of eq. (130) is represented in fig. 2 for three values of the quintessence parameter: our estimated value of  $N_q$ , along with lower and upper values. As expected, when  $x \rightarrow 1^+$  the logarithmic term becomes increasingly dominant, compressing the wave function oscillations and making the different  $N_q$  distinguishable only at extremely small distances.

The cloudless scenario is obtained by setting  $\bar{a} = 0$  in the above result. This happens because when  $\alpha_q = 0$ , both  $\bar{a}$  and  $N_q$  contribute identically to the metric function  $A(x)$ , given by eq. (25). An interesting particular case is the one where  $\epsilon^2 = (\bar{a} + N_q) \bar{m}_\phi^2$ , which simplifies eq. (130) to

$$R_{st}^{(0)}(x)/R_0 = \exp \left[ \pm i \frac{\epsilon \rho_s}{(\bar{a} + N_q)^2} \ln(x-1) \right],\tag{131}$$

determining the dark phase.

Alternatively, setting  $N_q = 0$  and  $\bar{a} \neq 0$  in eq. (25) describes a space-time devoid of quintessence, yet still containing the black string and string clouds. This configuration, valid for all  $\alpha_q$  provided  $\rho_+ \ll |l|$ , defines the free quintessence regime, given by eq. (42), which we will analyze in the sequence.

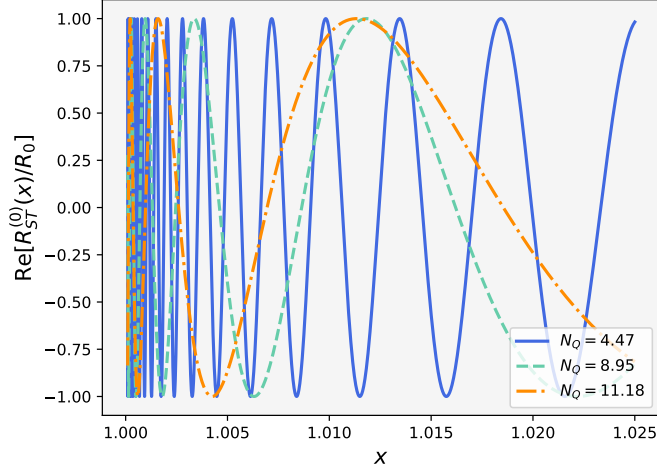


Figure 2: Real part of the non-normalized radial wave function ( $R_{ST}^{(0)}(x)$ ) as a function of the dimensionless radial coordinate  $x = \rho/\rho_+$  for the standard scenario of  $\alpha_Q = 0$ . This result is obtained from eq. (130). The parameters are fixed at  $\rho_S = 10^2$  m,  $\bar{a} = 10^{-3}$ ,  $\epsilon = n\bar{m}_\phi$ , with  $n = 4$ , and  $\bar{m}_\phi = 1$  m $^{-1}$  (chosen for visual clarity). For realistic values of  $\bar{m}_\phi = m_\phi c/\hbar$ , the oscillations would be much more rapid, making the distinction between different  $N_Q$  values visible only at extremely small distances. Furthermore, note that besides the compression of these oscillations as  $x \rightarrow 1^+$ , due to  $\ln(x-1)$ , the wavelength increases with increasing  $N_Q$ .

### 6.1.1. Free quintessence regime and contribution from string clouds

We now investigate the free quintessence regime, given by eq. (46). This regime is valid for all  $\alpha_Q$ , for a large domain of the radial coordinate as long as  $\rho_+ \ll |l|$ , as we mentioned before. Provided  $N_Q$  is set to zero, we know there will not exist any phase shift due to the quintessential fluid in the radial wave function. However, it is interesting that, in this case, we can directly explore the contribution from the string clouds. To do so, we consider a particle in the vicinity of the event horizon, where  $R_F(x)$  can be approximated as

$$R_F(x) = R_0 \exp\left[\frac{\gamma}{2} \ln(x-1) + \frac{\alpha}{2}\right], \quad (132)$$

where, again,  $R_0$  stands for a normalization constant. Note that the only difference between the wave functions (128) and (132) lie in the expressions for the Heun parameters  $\gamma$  and  $\alpha$ , besides  $R_0$  naturally. Since  $N_Q$  and  $\bar{a}$  have the same role in wave functions associated with  $\alpha_Q = 0$ , we do not need

to calculate the expression for the free quintessence regime. We can simply choose  $N_q = 0$  in our previous result (130), implying that:

$$R_F(x)/R_0 = \exp \left\{ \pm i \frac{\rho_s}{\bar{a}^2} \left[ \epsilon \ln(x-1) + \sqrt{\epsilon^2 - \bar{a} \bar{m}_\phi^2} \right] \right\}. \quad (133)$$

In the special case where  $\bar{a} \in \mathbb{R}^+$  satisfies  $\bar{a} \ll 1$ , we can use the Laurent series to expand  $\sqrt{\epsilon^2 - \bar{a} \bar{m}_\phi^2}/\bar{a}^2$  around  $\bar{a} = 0$ , to show that the real part of the radial wave function takes the form of

$$\text{Re}[R_F(x)/R_0] = \cos \left[ \frac{\epsilon \rho_s}{\bar{a}^2} \ln(x-1) + \theta_{\bar{a}} \right], \quad (134)$$

with

$$\theta_{\bar{a}} = |\epsilon| \rho_s \left( \frac{1}{\bar{a}^2} - \frac{\bar{m}_\phi^2}{2\bar{a} \epsilon^2} - \frac{\bar{m}_\phi^4}{8 \epsilon^4} - \frac{\bar{m}_\phi^6}{16 \epsilon^6} \bar{a} \right) + \mathcal{O}(\bar{a}^2).$$

showing the explicit dependence of  $R_F(x)$  in terms of  $\bar{a}$ . The imaginary part of this radial wave function would be identical to eq. (134) up to a  $\pi/2$  phase shift.

Finally, we could also impose the energy constraint  $\epsilon^2 = \bar{a} \bar{m}_\phi^2$  as a special case, which significantly simplifies eq. (133) to eq. (131) by setting  $N_q = 0$ . This is identical to setting  $\theta_{\bar{a}} = 0$  in eq. (134).

## 6.2. Dark phases for intermediate state parameter

When  $\alpha_q = 1/2$ , in the standard scenario, the radial wave function  $R_{ST}^{(1/2)}(x)$  is determined by eq. (61), with the Heun parameters specified by eq. (60). Near the event horizon, this radial wave function can be approximated as:

$$R_{ST}^{(1/2)}(x) = R_0 \left( 1 - \frac{N_q \rho_s}{\bar{a}^2} \right) \exp \left[ \frac{\gamma}{2} \ln(x-1) + \frac{\alpha}{2} \right], \quad (135)$$

where we used the result (A.34), with  $c_0 = 1$ , to describe the zeroth order approximation of the local confluent Heun function. Next, we recall that this solution is valid in the regime where  $N_q \rho_s / \bar{a}^2 \ll 1$ , implying the Heun parameters  $\gamma$  and  $\alpha$ , given by eq. (60), can be written as

$$\begin{aligned} \frac{\gamma}{2} &= \pm i \frac{\epsilon \rho_s}{\bar{a}^2} \left( 1 - \frac{2N_q \rho_s}{\bar{a}^2} \right), \\ \frac{\alpha}{2} &= \pm \frac{\epsilon \rho_s}{\bar{a}^2} \left( 1 + \frac{N_q \rho_s}{\bar{a}^2} \right). \end{aligned} \quad (136)$$

Therefore, near the horizon, the radial wave function behaves as

$$R_{ST}^{(1/2)}(x) = \Phi_{\pm} \exp [\mp i \delta_{ST}^{(1/2)}] , \quad (137)$$

where

$$\Phi_{\pm} = \bar{R}_0 \exp \left[ \pm i \frac{\epsilon \rho_s}{\bar{a}^2} \ln(x-1) \pm \frac{\epsilon \rho_s}{\bar{a}^2} \right] .$$

Here  $\bar{R}_0 = R_0 (1 - N_q \rho_s / \bar{a}^2)$ . Note that  $\Phi_{\pm}$  is independent of the quintessence parameter  $N_q$ , while  $\delta_{ST}^{(1/2)}$  is a phase shift caused by the presence of quintessence:

$$\delta_{ST}^{(1/2)} = [2 \ln(x-1) + i] \epsilon \frac{N_q \rho_s^2}{\bar{a}^4} . \quad (138)$$

This result is different from the one we had obtained for  $\alpha_q = 1/2$  in [36], because in the present study we investigate the particular case satisfying the energy constraint (57), namely  $\epsilon^2 = \bar{a} \bar{m}_{\phi}^2 / 2$ .

In addition to this standard case, we show an example of a dark phase occurring in the cloudless scenario for a massless spin-0 boson ( $\bar{m}_{\phi} = 0$ ), with  $\alpha_q = 1/2$ . In this situation, we consider the radial wave function  $R_{CL}^{(1/2, \Delta)}(x)$ , given by eqs. (74) and (76), as

$$R_{CL}^{(1/2, \Delta)}(x) = x^{-1/2} [c_1 x^{s/2} + c_2 x^{-s/2}] . \quad (139)$$

This expression is valid for the extended domain without any further approximations. Since  $\alpha_q = 1/2$ , it follows from table 1 that  $N_q \sim 10^{-26} \text{ m}^{-1}$ ; thus, the parameter  $s$ , defined by eq. (72), can be written as

$$\frac{s}{2} = i \frac{|\epsilon|}{N_q} \left( 1 - \frac{N_q^2}{\epsilon^2} \right) + \mathcal{O}(N_q^4) ,$$

implying that the radial function is

$$R_{CL}^{(1/2, \Delta)}(x) = \Phi_+(x) \exp [i \delta_{CL}^{(1/2, \Delta)}] + \Phi_-(x) \exp [-i \delta_{CL}^{(1/2, \Delta)}] , \quad (140)$$

where

$$\Phi_{\pm}(x) = c_{\pm} x^{-1/2}$$

while  $\delta_{CL}^{(1/2, \Delta)}(x)$  is

$$\delta_{CL}^{(1/2, \Delta)}(x) = \frac{|\epsilon|}{N_q} \left( 1 - \frac{N_q^2}{\epsilon^2} \right) \ln x . \quad (141)$$

Notably, this result is valid for a large domain in the coordinate  $x$ , that is, for all  $x$  satisfying  $x \rho_+ \ll |l|$ . In the restricted case where  $N_q \ll \epsilon$ , the phase shift  $\delta_{CL}^{(1/2, \Delta)}(x)$  simplifies to  $\delta_{CL}^{(1/2, \Delta)}(x) = (|\epsilon|/N_q) \ln x$ .

### 6.3. Dark phases at the upper bound

For  $\alpha_q = 1$ , we first examine the standard solution in the vicinity of the event horizon, as given by eq. (93). The explicit Heun parameters for this case, valid in the physical regime where  $N_{ql} \rho_s^2 / \bar{a}^3 \ll 1$ , are presented in eq. (94). This leads to the radial wave function:

$$R_{ST}^{(1)}(x) = \Phi_+(x) \exp[i \delta_{ST+}^{(1)}(x)] + \Phi_-(x) \exp[i \delta_{ST-}^{(1)}(x)] , \quad (142)$$

where the functions  $\Phi_{\pm}(x)$  and  $\delta_{ST\pm}^{(1)}(x)$  are defined as

$$\Phi_{\pm}(x) = c_{\pm} \exp \left[ \frac{i\epsilon\rho_s}{\bar{a}^2} \ln(x-1) \pm \left( \frac{1}{4} - \frac{\kappa^2}{\bar{a}} \right)^{1/2} (x-1) \right]$$

and

$$\delta_{ST\pm}^{(1)}(x) = - \left[ \frac{2\epsilon\rho_s}{\bar{a}^2} \ln(x-1) \pm i \left( \frac{1}{4} - \frac{\kappa^2}{\bar{a}} \right)^{-1/2} \frac{\kappa^2}{\bar{a}} (x-1) \right] \frac{N_{ql} \rho_s^2}{\bar{a}^3} . \quad (143)$$

Once again, the presence of the parameter  $N_q$  in eq. (143) demonstrates how quintessence induces a phase shift in the radial wave function, whereas  $\Phi_{\pm}$  is independent of it. We give numerical examples of this scenario in figs. 3 and 4, where we explore the behavior of the real part of  $R_{ST}^{(1)}(x)$ , given by eq. (142), for varying values of  $\epsilon$  and  $N_q$ , respectively.

It is crucial to recall that the results derived from eq. (93) represent accurate approximations solely within the restricted domain of  $x \rightarrow 1^+$ , and if we are interested in extending the domain (for the radial coordinate) we should introduce corrections to these dark phases. However, the key observation remains: even near the event horizon, a phase shift emerges due to quintessence. Given that the contribution of the quintessence term ( $N_q \rho^{2\alpha_q}$ ) to the metric function  $A(\rho)$  increases with  $\rho$ , we anticipate a more pronounced phase shift at larger distances. This expectation aligns with the results for  $R_{ST}^{(1)}(x)$  at large  $x$ , as determined by eqs. (101) and (102). Nonetheless, we defer a detailed numerical investigation of this aspect to future work.

In the cloudless scenario with  $\alpha_q = 1$ , the radial wave function of the scalar particle, valid for  $x \rightarrow 1^+$  (near the horizon), is given by eq. (22), while the Heun parameters  $\gamma$  and  $\beta$  are explicitly given by eq. (109). Note that, with  $\rho_s$  ranging from  $10^{-2}$  m to  $10^{15}$  m, while  $N_{ql} \sim 10^{-52} \text{ m}^{-2}$  (please,

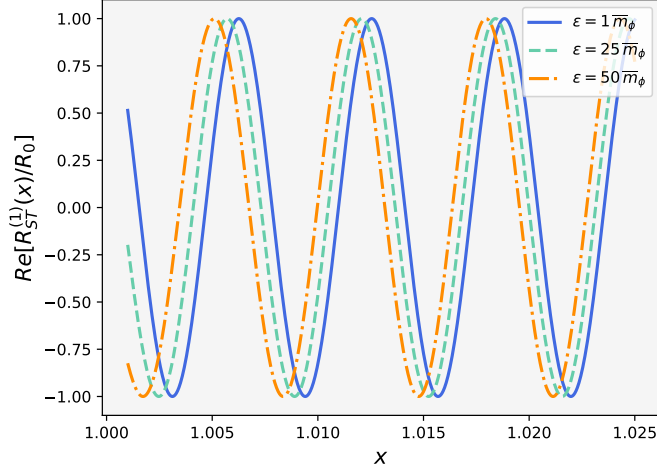


Figure 3: Real part of the radial wave function  $R_{ST}^{(1)}(x)$  near the event horizon (derived from eqs. (142) and (143), with  $c_+ = 0$  and  $c_- = R_0$ ), as a function of the dimensionless radial coordinate  $x = \rho/\rho_+$  for the standard scenario of  $\alpha_Q = 1$  (the upper bound). The different curves correspond to various values of  $\epsilon$ . We considered  $N_Q = 10^{-52} \text{ m}^{-2}$ ,  $\kappa = 1$  (indicating the particle does not move along the  $z$ -axis),  $\rho_S = 2 \times 10^{10} \text{ m}$ , and  $\bar{a} = 10^{-6}$ . The parameter  $\bar{m}_\phi$  was set to  $\bar{m}_\phi = 2.23 \times 10^{-25} \text{ m}^{-1}$  for visual clarity; realistic values of  $\bar{m}_\phi$  would require us infinitely smaller distances to discern the phase shift.

see table 1), it follows that  $(N_{QL} \rho_S^2)^{1/3} \ll 1$ . Then, recalling that  $\kappa$ , defined by eq. (11b), is  $\kappa^2 = n_R^2 + k_z^2$ , where  $n_R \in \mathbb{Z}$  and  $k_z$  is related to the particle's momentum along the  $z$ -axis, we can expand the  $\beta$  parameter as

$$\frac{\beta}{2} = \pm \frac{i}{\sqrt{3}} \frac{\kappa}{(N_{QL} \rho_S^2)^{1/6}}.$$

Using the result above, along with the  $\gamma$  parameter expressed in eq. (109), the radial wave function  $R_{CL}^{(1)}(x)$  can be written as

$$R_{CL}^{(1)}(x) = c_+ \exp[i \delta_{CL+}^{(1)}(x)] + c_- \exp[i \delta_{CL-}^{(1)}(x)],$$

with

$$\delta_{CL\pm}^{(1)}(x) = \left[ \frac{\epsilon}{3 N_{QL}^{1/2}} \ln(x-1) \pm \frac{\kappa}{\sqrt{3}} (x-1) \right] (N_{QL} \rho_S^2)^{-1/6}. \quad (144)$$

Clearly, the term containing  $\ln(x-1)/N_{QL}^{1/2}$  dominates the dark phase (144).

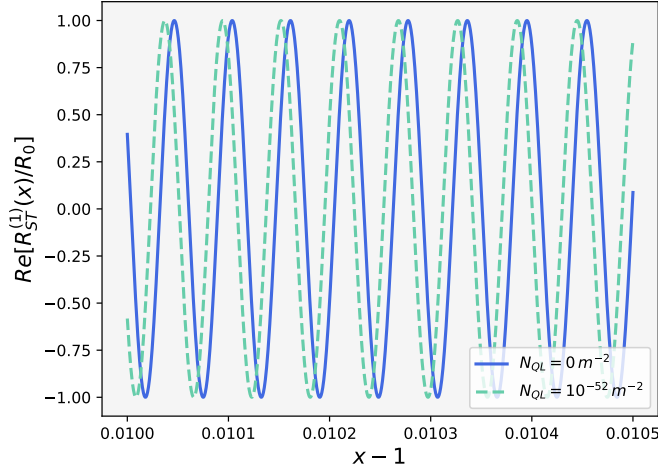


Figure 4: Real part of the radial wave function  $R_{ST}^{(1)}(x)$ , given by eqs. (142) and (143) (with  $c_+ = 0$  and  $c_- = R_0$ ), as a function of the dimensionless distance from the event horizon  $x - 1$ . The figure represents the standard scenario of  $\alpha_q = 1$  (the upper bound) near the event horizon. We considered  $\kappa = 1$ , implying the particle does not move in the vertical direction. The remaining parameters are  $\rho_S = 10^{15}$  m,  $\bar{a} = 10^{-6}$ ,  $\bar{m}_\phi = 2.23 \times 10^{-25}$  m $^{-1}$  (chosen for visual clarity), and  $\epsilon = 5 \bar{m}_\phi$ . The two curves illustrate the cases with  $N_{QL} = 0$  m $^{-2}$  (absence of quintessence) and  $N_{QL} = 10^{-52}$  m $^{-2}$  (presence of quintessence). Notably, a quintessence-induced phase shift distinguishes a particle in the presence of dark energy. As with previous figures, a convenient value for  $\bar{m}_\phi$  was used, as realistic values would imply the phase shift would be noticeable only at much smaller distances.

#### 6.4. Horizonless scenarios

The extended solutions presented in this work reveal another intriguing feature: the ability to obtain solutions for horizonless cases by setting  $\rho_S = 0$ . This was demonstrated in sections 3.2, 4.2 and 5.4. We now proceed to analyze these radial wave functions.

For  $\alpha_q = 0$ , the radial wave function in the horizonless regime can be expressed using the confluent Heun function, as detailed in eq. (37), or in terms of Bessel functions, as given by eq. (41). To illustrate the utility of the Bessel function solution, we expand  $R_{HL}^{(0)}(\rho)$ , with  $c_2 = 0$  around  $\rho = 0$  to examine the influence of quintessence on the wave function. This yields:

$$R_{HL}^{(0)}(\rho) = \bar{R}_0 \rho^{-1/2} \exp[i \delta_{HL}^{(0)}], \quad (145)$$

where

$$\overline{R}_0 = c_1 \frac{2^{-m} k^m}{\Gamma(m+1)} \exp[-im(k+\pi)] .$$

Here,  $c_1$  is the normalization constant,  $\Gamma(m+1)$  is the standard Gamma function [51, 49], and  $k$  and  $m$  are defined by eqs. (39) and (40), respectively. The dark phase associated with the term  $\exp(i\delta_{HL})$  is given by

$$\delta_{HL}^{(0)} = \sqrt{\frac{1}{4} + \frac{\kappa^2}{\bar{a} + N_q}} (\rho - i \ln \rho) . \quad (146)$$

We choose not to expand the square root in eq. (146) as  $N_q$  is not small within this regime; specifically, we expect  $N_q$  to be close to 8.95, in accordance with table 1, when  $\alpha_q = 0$ . In figs. 5 and 6, we show the behavior of  $R_{HL}^{(0)}(\rho)/\overline{R}_0$ , defined by eq. (145), for different values of the quintessence parameter  $N_q$ , from  $N_q = 0$  (absence of quintessence) to  $N_q = 8.95$  (our estimate from table 1). It is relevant to note that fig. 5 is associated with the approximation near the origin, given by eq. (146), while fig. 6 is valid for the whole radial domain, as determined by eq. (41), where the amplitude of  $R_{HL}^{(0)}(\rho)$  correctly diminishes with the increase of the radial distance  $\rho$ .

Having examined the  $\alpha_q = 0$  case, we now turn our attention to the horizonless scenario with  $\alpha_q = 1/2$ . The radial wave function for the extended domain is given by eq. (81), subject to the constraint  $\epsilon^2 = \bar{a} \bar{m}_\phi^2/2$ . However, to analyze its behavior near the origin, we use the approximation from eq. (83), namely:

$$R_{HL}^{(1/2)}(\rho) \approx (\rho - 1)^{(1+\gamma)/2} \left[ c_1 \rho^{(\beta-1)/2} + c_2 \rho^{-(\beta+1)/2} \right] .$$

Note that the Heun parameters  $\gamma$  and  $\beta$ , defined by eq. (80), are independent of  $N_q$ , indicating that this radial wave function does not exhibit a dark phase near the origin. But, from eqs. (80) and (81), we see that a dark phase might emerge at larger radial distances, where the quintessence contribution to the metric function becomes significant. Nevertheless, we defer this numerical investigation to future work.

To conclude our analysis, we investigate the horizonless scenario with  $\alpha_q = 1$ . The radial wave function for the extended domain, as given by eq. (122), is:

$$R_{HL}^{(1)}(z) = \frac{R_0}{z} \left[ 1 - \frac{N_{qL}}{2\bar{a}} \frac{z^2}{(2P)^{1/2}} \right] z^{(1+\alpha)/2} e^{-z^2/2} \text{HeunB}(\alpha, \beta, \gamma, \delta; z) .$$

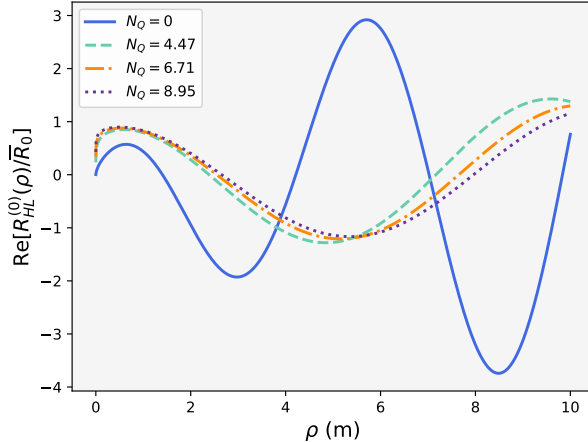


Figure 5: Real part of the radial wave function  $R_{HL}^{(0)}(\rho)$  (given by eqs. (145) and (146)) in the horizonless scenario of  $\alpha_q = 0$ , for various values of the quintessence parameter  $N_Q$ . Since there is no event horizon, this behavior is valid near the origin (at  $\rho = 0$ ). For simplicity, we chose  $\kappa = 1$ , which describes a spin-0 particle moving in a plane of fixed  $z = z_0$ . The other parameters are set to  $\rho_S = 10^5$  m,  $\bar{a} = 1$ ,  $\bar{m}_\phi = 1$  m $^{-1}$ ,  $\epsilon = 4\bar{m}_\phi$ . As with the previous figures,  $\bar{m}_\phi$  is chosen to facilitate the visualization.

This solution is valid provided  $2\epsilon^2 - \bar{a}\bar{m}_\phi^2 \neq 0$ . The Heun parameters for this regime are defined by eq. (121), while  $P$  (which depends on  $N_{qL}$ ) is defined by eq. (119), and the auxiliary variable  $z$  is given by  $z = (2P)^{1/4}\rho$ .

Furthermore, it is crucial to emphasize that, in this regime, all the the Heun parameters, given by eq. (121), are independent of  $N_{qL}$ . Consequently,  $\text{HeunB}(\alpha, \beta, \gamma, \delta; z)$  is entirely independent of the quintessence parameter. It is also true that the solution  $R_{HL}^{(1)}(z)$  holds for all  $z > 0$  (or, equivalently,  $\rho > 0$ ) due to the inclusion of the  $1/l^2$  term in the  $\alpha_q = 1$  solutions.

Therefore, the only contribution from quintessence to  $R_{HL}^{(1)}(z)$  is through the factor

$$1 - \frac{N_{qL}}{2\bar{a}} \frac{z^2}{(2P)^{1/2}} = 1 - \frac{N_{qL}}{2\bar{a}} \rho^2. \quad (147)$$

In summary, this radial wave function does not exhibit a “dark phase” but does experience an overall modification due to quintessence. This modification approaches zero as  $\rho \rightarrow 0$ , but it may become detectable at larger values of  $\rho$ . As expected, our dark energy candidate primarily influences the

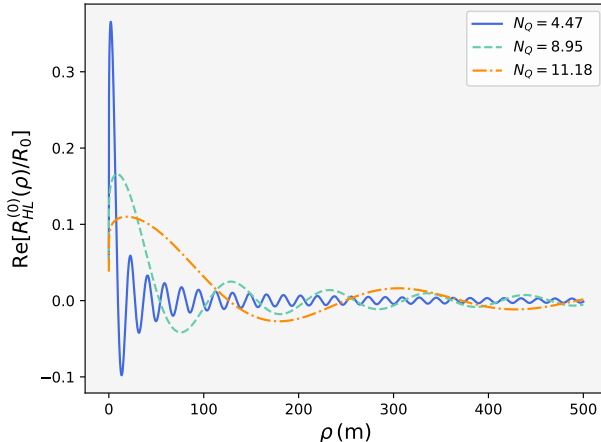


Figure 6: Real part of the exact solution  $R_{HL}^{(0)}(\rho)$ , given by eq. (41) (with  $c_1 = R_0$  and  $c_2 = 0$ ), valid for the extended radial domain where  $\rho$  is much smaller than the AdS radius  $l$ . This figure complements fig. 5, which describes the horizonless scenario of  $\alpha_Q = 0$  near the origin. For consistency with fig. 5, we used  $\kappa = 1$ ,  $\rho_S = 10^5$  m,  $\bar{a} = 1$ ,  $\bar{m}_\phi = 1$  m $^{-1}$ ,  $\epsilon = 4\bar{m}_\phi$ . Note that the oscillation frequency decreases with increasing values of  $N_Q$ .

solution at large distances.

Our final task is to investigate the remaining particular case when  $\epsilon^2 = \bar{a}\bar{m}_\phi^2/2$ . The associated radial wave function for  $\alpha_Q = 1$  is given by eq. (127), where the order  $n$  of the modified Bessel functions is defined by eq. (86). Notably, we observe directly from eq. (127) that  $R_{HL}^{(1,\otimes)}(\rho)$  exhibits the same overall quintessence-induced effect as in the previous case (cf. eq. (147)). Specifically, as  $\rho \rightarrow 0$  the effect becomes null, and it increases for larger values of  $\rho$ .

## 7. Conclusion

Understanding the intricate interplay between quantum phenomena and the nature of dark energy is of the highest importance for a comprehensive understanding of our universe. In this study, we have extended our previous analysis [36] of the Klein-Gordon equation for a scalar particle within a black string spacetime immersed in anisotropic quintessence fluid, and surrounded by a cloud of strings. Our investigation focused on exploring the influence of

the quintessence state parameter,  $\alpha_q$ , on the radial wave functions and the emergence of “dark phases”.

For  $\alpha_q = 0$  and  $\alpha_q = 1/2$ , we obtained solutions valid for a large radial domain, revealing that the quintessence contribution significantly affects the wave function, especially at larger distances. Notably, for  $\alpha_q = 1$ , the domain was unrestricted, highlighting the combined influence of quintessence and the cosmological constant. This regime of  $\alpha_q = 1$  is of great importance, even within our hypothetical cylindrical universe. These solutions allow for valuable comparisons with the realistic case of spherical symmetry, for which we have recent observational constraints [21, 22, 23, 24].

Building upon these solutions, we have demonstrated the existence of quintessence-induced phase shifts in the radial wave functions for the black string scenarios (both standard and cloudless). We termed them “dark phases” since they are directly associated with the quintessence parameter  $N_q$ . These phases are particularly evident near the event horizon.

Moreover, our extension to horizonless scenarios revealed that, while dark phases are usually absent near the origin (except for eq. (146)), quintessence still influences the overall radial wave function, particularly at larger distances. This effect is consistent with our knowledge that dark energy predominantly affects physics at large scales. But at the same time, it is intriguing how this extension to horizonless cases differed from our expectations for dark phases. These results suggest the event horizon plays a critical role in the quintessence-induced phase shifts.

To further illustrate our findings, we have included numerical examples demonstrating the effect of quintessence on the radial wave functions of a spin-0 particle. These are shown in figs. 2–4 for standard black string scenarios, and in figs. 5 and 6 for horizonless scenarios.

In summary, our findings contribute to a deeper understanding of the potential influence of dark energy on quantum phenomena. Future numerical studies are necessary to further explore our current results and their theoretical predictions.

## Acknowledgments

M.L.D. gratefully acknowledges Sophie Ashworth for insightful discussions. M.L.D. also acknowledges the Coordenação de Aperfeiçoamento de Pessoal de Nível Superior – Brasil (CAPES) for financial support, under Finance Code 001. B.V.S. and C.C.B.Jr. acknowledge the National Council for

Scientific and Technological Development (CNPq, Brazil) for their financial support. Specifically, B.V.S. thanks CNPq for grant number 141549/2023-8.

## Appendix A. Fuchs-Frobenius solution to the confluent Heun equation

Let us consider the canonical form of the confluent Heun equation, given by [40, 43]:

$$\frac{d^2 y}{dz^2} + \left( \alpha + \frac{\beta + 1}{z} + \frac{\gamma + 1}{z - 1} \right) \frac{dy}{dz} + \left( \frac{\mu}{z} + \frac{\nu}{z - 1} \right) y = 0, \quad (\text{A.1})$$

with  $z = 0, 1$  being the regular singular points. The irregular singular point lies at infinity. For the case of the standard confluent Heun *function*, it is true that

$$\text{HeunC}(\alpha, \beta, \gamma, \delta, \eta; 0) = 1, \quad (\text{A.2})$$

while

$$\mu = \frac{1}{2}(\alpha - \beta - \gamma + \alpha\beta - \beta\gamma) - \eta, \quad (\text{A.3})$$

$$\nu = \frac{1}{2}(\alpha + \beta + \gamma + \alpha\gamma + \beta\gamma) + \delta + \eta. \quad (\text{A.4})$$

### Appendix A.1. Liouville normal form

It is quite useful to rewrite eq. (A.1) in the Liouville normal form. To obtain the general expression, let us consider that

$$y(z) = I(z) u(z), \quad (\text{A.5})$$

so that any second-order linear differential equation of the form

$$y''(z) + p(z)y'(z) + q(z)y(z) = 0 \quad (\text{A.6})$$

can be written as

$$\begin{aligned} 0 &= I(z) u''(z) + [2I'(z) + p(z)I(z)] u'(z) \\ &+ [I''(z) + p(z)I'(z) + q(z)I(z)] u(z). \end{aligned} \quad (\text{A.7})$$

Demanding that the term associated with the first derivative of  $u(z)$  be zero, we see that

$$I'(z) = -\frac{1}{2}p(z)I(z), \quad (\text{A.8})$$

so that

$$I(z) = I_0 \exp\left(-\frac{1}{2} \int_{z_0}^z p(z') dz'\right). \quad (\text{A.9})$$

Hence, as long as  $I(z) \neq 0$ , the ODE for  $u(z)$  can be written as:

$$u''(z) + \left[ \frac{I''(z)}{I(z)} + p(z) \frac{I'(z)}{I(z)} + q(z) \right] u(z) = 0. \quad (\text{A.10})$$

Then, we use the result of eq. (A.8) to show that eq. (A.10) reads

$$u''(z) + \left[ -\frac{1}{2}p'(z) - \frac{1}{4}p(z)^2 + q(z) \right] u(z) = 0. \quad (\text{A.11})$$

Next, comparing the confluent Heun equation from (A.1) with the general second-order linear ODE from eq. (A.6), we identify that

$$p(z) = \alpha + \frac{\beta + 1}{z} + \frac{\gamma + 1}{z - 1}, \quad (\text{A.12})$$

$$q(z) = \frac{\mu}{z} + \frac{\nu}{z - 1}. \quad (\text{A.13})$$

It can be shown that the above expression for  $p(z)$  when applied to eq. (A.9) implies  $y(z)$  has the form

$$y(z) = y_0 e^{-\alpha z/2} z^{-(1+\beta)/2} (z - 1)^{-(1+\gamma)/2} u(z), \quad (\text{A.14})$$

where  $y_0$  is a constant. Plugging the expression for  $p(z)$ , given by (A.12), into eq. (A.11) it follows that

$$u''(z) + \left[ \frac{A}{z} + \frac{B}{(z - 1)} + \frac{C}{z^2} + \frac{D}{(z - 1)^2} + E \right] u(z) = 0, \quad (\text{A.15})$$

with

$$\begin{aligned} A &= \frac{1}{2} - \eta, \\ B &= -\frac{1}{2} + \delta + \eta, \\ C &= (1 - \beta^2)/4, \\ D &= (1 - \gamma^2)/4, \\ E &= -\alpha^2/4. \end{aligned} \quad (\text{A.16})$$

Therefore, any ODE of the form (A.15) will have the following solution:

$$\begin{aligned} u(z) &= e^{\alpha z/2} z^{(1+\beta)/2} (z - 1)^{(1+\gamma)/2} [c_1 \text{HeunC}(\alpha, \beta, \gamma, \delta, \eta; z) \\ &\quad + c_2 z^{-\beta} \text{HeunC}(\alpha, -\beta, \gamma, \delta, \eta; z)], \end{aligned} \quad (\text{A.17})$$

where  $c_1, c_2$  are arbitrary constants to be set with boundary conditions.

*Appendix A.2. Frobenius method*

In the sequence, we can investigate the Frobenius solution to eq. (A.1). We start by considering that

$$y(z) = \sum_{k=0}^{+\infty} c_k z^{r+k}. \quad (\text{A.18})$$

These derivatives are given by:

$$\begin{aligned} y'(z) &= \sum_{k=0}^{+\infty} (r+k) c_k z^{r+k-1}, \\ y''(z) &= \sum_{k=0}^{+\infty} (r+k)(r+k-1) c_k z^{r+k-2}. \end{aligned} \quad (\text{A.19})$$

Now, we multiply eq. (A.1) by  $z(z-1)$  and plug the results (A.18) and (A.19) into it. This results in:

$$\begin{aligned} 0 &= \sum_{k=0}^{+\infty} c_k [(k+r)(k+r+\Delta_c-1) - \mu] z^{k+r} \\ &\quad - \sum_{k=0}^{+\infty} c_k [(k+r)(k+r+\beta)] z^{k+r-1} \\ &\quad + \sum_{k=0}^{+\infty} c_k [(k+r)\alpha + (\mu+\nu)] z^{k+r+1}, \end{aligned} \quad (\text{A.20})$$

where

$$\Delta_c = \beta + \gamma - \alpha + 2. \quad (\text{A.21})$$

Afterward, we recall that

$$\begin{aligned} \sum_{k=0}^{+\infty} c_k [(k+r)(k+r+\beta)] z^{k+r-1} &= c_0 r(r+\beta) z^{r-1} \\ &\quad + \sum_{k=0}^{+\infty} c_{k+1} [(k+r+1)(k+r+1+\beta)] z^{k+r}. \end{aligned} \quad (\text{A.22})$$

On the other hand,

$$\sum_{k=0}^{+\infty} c_k [(k+r)\alpha + (\mu+\nu)] z^{k+r+1} = \sum_{k=1}^{+\infty} c_{k-1} [(k+r-1)\alpha + (\mu+\nu)] z^{k+r}. \quad (\text{A.23})$$

Thus, we plug the expressions (A.22) and (A.23) into eq. (A.20) to see that

$$\begin{aligned}
& -c_0 r(r+\beta)z^{r-1} + c_0 [r(r+\Delta_c-1) - \mu]z^r - c_1(r+1)(r+1+\beta)z^r \\
& + \sum_{k=1}^{\infty} \{c_{k-1}[(k+r-1)\alpha + (\mu + \nu)] + c_k[(k+r)(k+r+\Delta_c-1) - \mu]\}z^{k+r} \\
& - \sum_{k=1}^{+\infty} c_{k+1}[(k+r+1)(k+r+1+\beta)]z^{k+r} = 0.
\end{aligned} \tag{A.24}$$

Since the coefficients of each power of  $z$  must be zero, and considering that  $c_0 = 1$ , we conclude that:

- a)  $r(r+\beta) = 0$ , which is the indicial equation;
- b)  $c_1 = [r(r+\Delta_c-1) - \mu] / [(r+1)(r+1+\beta)]$ , determining the coefficient  $c_1$ .
- c) The general term is given by

$$\begin{aligned}
c_{k+1}[(k+r+1)(k+r+1+\beta)] &= c_{k-1}[(k+r-1)\alpha + (\mu + \nu)] \\
&+ c_k[(k+r)(k+r+\Delta_c-1) - \mu],
\end{aligned}$$

for  $k \geq 1$ . Note that we can rewrite the general term after a shift in  $k = m+1$ , resulting in:

$$\begin{aligned}
c_{m+2}[(m+r+2)(m+r+2+\beta)] &= c_m[(m+r)\alpha + (\mu + \nu)] \\
&+ c_{m+1}[(m+r+1)(m+r+\Delta_c) - \mu],
\end{aligned}$$

with  $m \geq 0$ . Since the parameters  $\mu$  and  $\nu$  are defined in terms of  $\alpha, \beta, \gamma, \delta$  and  $\eta$ , we can write alternative expressions for the factors multiplying  $c_{m+2}$ ,  $c_{m+1}$  and  $c_m$ . First, we use eqs. (A.3) and (A.4) to obtain that

$$\mu + \nu = \frac{\alpha}{2}(\beta + \gamma + 2) + \delta. \tag{A.25}$$

In the sequence, we consider that eq. (A.3) can be written as

$$\mu = -\frac{\beta}{2} - \eta + \frac{1}{2}(\alpha - \gamma)(1 + \beta). \tag{A.26}$$

Hence, the general term for the recursion relation becomes

$$A_2 c_{m+2} = A_0 c_m + A_1 c_{m+1}, \quad m \geq 0, \quad (\text{A.27a})$$

where

$$A_0 = (m+r)\alpha + \frac{\alpha}{2}(\beta + \gamma + 2) + \delta, \quad (\text{A.27b})$$

$$A_1 = \frac{\beta}{2} + \eta - \frac{1}{2}(\alpha - \gamma)(1 + \beta) + (m+r+1)(m+r + \Delta_c), \quad (\text{A.27c})$$

$$A_2 = (m+r+2)(m+r+2 + \beta), \quad (\text{A.27d})$$

according to the results (A.25), (A.26) and also (A.21).

As an example, we provide the first coefficients of the Fuchs-Frobenius solution below:

$$\begin{aligned} c_0 &= 1, \\ c_1 &= \frac{r(r + \Delta_c - 1) - \mu}{(r+1)(r+1 + \beta)}, \end{aligned} \quad (\text{A.28})$$

while

$$c_2 = \frac{\frac{\alpha}{2}(2r + \beta + \gamma + 2) + \delta}{(r+2)(r+2 + \beta)} + \left[ \frac{(r+1)(r + \Delta_c) - \mu}{(r+2)(r+2 + \beta)} \right] \left[ \frac{r(r + \Delta_c - 1) - \mu}{(r+1)(r+1 + \beta)} \right]. \quad (\text{A.29})$$

Setting  $r = 0$  first, and then  $r = -\beta$  gives us the terms of the two linearly independent Fuchs-Frobenius solutions up to the second order in  $z$ . In future approximations, we shall consider the approximation to the zeroth order only.

### *Appendix A.2.1. Series break-off*

In physical applications, finding polynomial solutions of Heun-type equations, such as the confluent Heun equation, can be valuable. These solutions can be derived from the Fuchs-Frobenius result, given by eqs. (A.27a)–(A.27d), by establishing that for some  $m = N \geq 0$ ,  $A_0 = 0$  as well as  $c_{m+1}(\alpha, \beta, \gamma, \delta, \eta) = 0$ . These constraints lead to an  $N$ -th degree polynomial that satisfies the confluent Heun equation, where the condition

$$\alpha \left( N + 1 + \frac{\beta + \gamma}{2} \right) + \delta = 0, \quad N \in \mathbb{Z}^+, \quad (\text{A.30})$$

known as the  $\delta$ -condition, must be met.

*Appendix A.3. Fuchs-Frobenius solution near  $z=1$*

Previously, we examined *local* Heun solutions near  $z = 0$ , with  $|z| < 1$ . However, this section investigates solutions near  $z = 1$  when a particle is close to the event horizon. To do this, consider the confluent Heun equation given by (A.1). First, we multiply eq. (A.1) by a factor of  $z(z - 1)$  so that

$$\begin{aligned} 0 &= z(z - 1)y''(z) \\ &+ [\alpha z(z - 1) + (\beta + 1)(z - 1) + (\gamma + 1)z]y'(z) \\ &+ [\mu(z - 1) + \nu z]y(z). \end{aligned} \quad (\text{A.31})$$

Next, let us define the auxiliary variable  $\chi := z - 1$ , such that

$$\frac{d}{d\chi} = \frac{d}{dz}.$$

In terms of  $\chi$ , eq. (A.31) becomes

$$\begin{aligned} 0 &= \chi^2 y'' + \Theta_c \chi y' + \nu y \\ &+ \chi y'' + (\gamma + 1) y' \\ &+ \alpha \chi^2 y' + (\mu + \nu) \chi y, \end{aligned} \quad (\text{A.32})$$

where

$$\Theta_c := \alpha + \beta + \gamma + 2, \quad (\text{A.33})$$

while the prime notation ( $'$ ) means a derivative with respect to  $\chi$ , i.e.  $d/d\chi$ .

Subsequently, we substitute the ansatz

$$y(\chi) = \sum_{m=0}^{+\infty} c_m \chi^{m+r}, \quad (\text{A.34})$$

into eq. (A.32) to demonstrate that

$$\begin{aligned} 0 &= \sum_{m=0}^{+\infty} c_m [(m + r)(m + r + \Theta_c - 1) + \nu] \chi^{m+r} \\ &+ \sum_{m=0}^{+\infty} c_m (m + r)(m + r + \gamma) \chi^{m+r-1} \\ &+ \sum_{m=0}^{+\infty} c_m [\alpha(m + r) + (\mu + \nu)] \chi^{m+r+1}. \end{aligned} \quad (\text{A.35})$$

Now, we rename the summation index  $m$  in eq. (A.35) to

- $k = m$  in the first sum;
- $k = m - 1$  in the second one;
- $k = m + 1$  in the last case.

By doing so, we obtain that

$$\begin{aligned}
0 &= \sum_{k=0}^{+\infty} c_k [(k+r)(k+r+\Theta_c-1)+\nu] \chi^{k+r} \\
&+ \sum_{k=-1}^{+\infty} c_{k+1} (k+r+1)(k+r+\gamma+1) \chi^{k+r} \\
&+ \sum_{k=1}^{+\infty} c_{k-1} [\alpha(k+r-1)+(\mu+\nu)] \chi^{k+r}.
\end{aligned} \tag{A.36}$$

It follows from eq. (A.36) that:

$$c_0 r (r + \gamma) = 0, \tag{A.37a}$$

$$c_1 = \frac{r(r+\alpha+\beta+\gamma+1)+\nu}{(r+1)(r+\gamma+1)} c_0, \tag{A.37b}$$

while we write the general term as

$$M_0 c_m + M_1 c_{m+1} + M_2 c_{m+2} = 0, \quad m \geq 0, \tag{A.37c}$$

with

$$M_0 = \alpha(m+r) + (\mu+\nu), \tag{A.37d}$$

$$M_1 = (m+r+1)(m+r+\alpha+\beta+\gamma+2) + \nu, \tag{A.37e}$$

$$M_2 = (m+r+2)(m+r+\gamma+2). \tag{A.37f}$$

Note that we wrote the final result in terms of  $m = k - 1$  for convenience. Also, one can describe the terms in eqs. (A.37d)–(A.37f) in an analogous way to what we did in eqs. (A.27b)–(A.27d) for the local solutions near  $z = 0$ . Doing so, we obtain an equivalent way to write  $M_0$ ,  $M_1$ , and  $M_2$  according to which:

$$M_0 = \alpha(m+r+1) + \frac{\alpha}{2}(\beta+\gamma) + \delta,$$

$$M_1 = (m+r+1)(m+r+\alpha+\beta+\gamma+2) + \frac{\gamma}{2} + \delta + \eta + \frac{1}{2}(\alpha+\beta)(1+\gamma),$$

$$M_2 = (m+r+2)(m+r+\gamma+2),$$

where we used (A.4) to write  $\nu$  as

$$\nu = \frac{\gamma}{2} + \delta + \eta + \frac{1}{2}(\alpha + \beta)(1 + \gamma). \quad (\text{A.38})$$

Finally, we can set  $c_0 = 1$  to obtain explicitly the first three coefficients of the local solution to the confluent Heun equation near  $z = 1$ , given by

$$\text{HeunCl}(\alpha, \beta, \gamma, \delta, \eta; z - 1) = 1 + c_1(z - 1) + c_2(z - 1)^2 + \dots, \quad (\text{A.39})$$

where

$$c_1 = \frac{r(r + \alpha + \beta + \gamma + 1)}{(r + 1)(r + \gamma + 1)} + \frac{(\alpha + \beta)(1 + \gamma) + \gamma + 2(\delta + \eta)}{2(r + 1)(r + \gamma + 1)}, \quad (\text{A.40})$$

and

$$c_2 = -\frac{1}{(r + 2)(r + \gamma + 2)} \left\{ \frac{\alpha}{2} (2r + \beta + \gamma + 2) + \delta \right. \\ \left. + c_1 \left[ (r + 1)(r + \alpha + \beta + \gamma + 2) + \frac{\gamma}{2} + \delta + \eta + \frac{1}{2}(\alpha + \beta)(1 + \gamma) \right] \right\}. \quad (\text{A.41})$$

### *Appendix A.3.1. Imposing the break off of the series solution*

According to the solution given by eqs. (A.37a)–(A.37f), one can demand the break off of the series (A.34) into a polynomial requiring that  $M_0 = 0$  and  $c_{m+1}(\alpha, \beta, \gamma, \delta, \eta) = 0$  for some  $m = N$ .

The first requirement, i.e.  $M_0 = 0$  for some  $m = N \in \mathbb{Z}^+$ , gives us the condition

$$\alpha \left( N + 1 + \frac{\beta + \gamma}{2} \right) + \delta = 0. \quad (\text{A.42})$$

However, note that the above condition is identical to (A.30), which is the one we have obtained for local solutions near  $z = 0$ .

## **Appendix B. Biconfluent Heun equation**

The canonical form of the Biconfluent Heun equation is defined as

$$\frac{d^2 y}{dz^2} + \left( \frac{1 + \alpha}{z} - \beta - 2z \right) \frac{dy}{dz} + \left\{ (\gamma - \alpha - 2) - \frac{[\delta + (1 + \alpha)\beta]/2}{z} \right\} y(z) = 0, \quad (\text{B.1})$$

where  $y(z) = \text{HeunB}(\alpha, \beta, \gamma, \delta; z)$ . To write eq. (B.1) in the normal form, we use the prescription given by eqs. (A.6), (A.9) and (A.11), to obtain the function  $I_B(z)$  relating the Biconfluent Heun equations with its normal form:

$$I_B(z) = \exp \left[ -\frac{1}{2} \int_{z_0}^z \left( \frac{1+\alpha}{z'} - \beta - 2z' \right) dz' \right],$$

which simplifies to

$$I_B(z) = I_0 z^{-(1+\alpha)/2} e^{\beta z/2} e^{z^2/2}. \quad (\text{B.2})$$

The resultant equation in the Liouville normal form becomes

$$u''(z) + \left[ A z^2 + B z + C + \frac{D}{z} + \frac{E}{z^2} \right] u(z) = 0, \quad (\text{B.3})$$

where now the parameters  $A, B, C, D$ , and  $E$  are given by

$$\begin{aligned} A &= -1/2, \\ B &= -\beta, \\ C &= \gamma - \beta^2/4, \\ D &= -\delta/2, \\ E &= (1 - \alpha^2)/4. \end{aligned} \quad (\text{B.4})$$

Therefore, the solution to any equation like (B.3) is of the form

$$u(z) = u_0 z^{(1+\alpha)/2} e^{-\beta z/2} e^{-z^2/2} \text{HeunB}(\alpha, \beta, \gamma, \delta; z). \quad (\text{B.5})$$

#### *Appendix B.1. Frobenius method applied to the biconfluent case*

Let us investigate the solution of the biconfluent Heun equation employing the Frobenius method. Let us recall that, by construction, the solution must be in the form of eq. (A.18), where its derivatives are given by (A.19). Next, multiplying (B.1) by  $z^2$  and plugging the ansatz into the ordinary differential equation, we obtain that

$$\begin{aligned} 0 &= \sum_{k=0}^{+\infty} c_k (k+r)(k+r-1) z^{k+r} \\ &+ \sum_{k=0}^{+\infty} c_k \left[ (1+\alpha)z - \beta z^2 - 2z^3 \right] (k+r) z^{k+r-1} \\ &+ \sum_{k=0}^{+\infty} c_k \left[ (\gamma - \alpha - 2)z^2 - \frac{1}{2}(\delta + \beta + \alpha\beta) \right] z^k + r. \end{aligned}$$

Now, we can organize the terms as follows:

$$\begin{aligned}
0 &= \sum_{k=0}^{+\infty} c_k (k+r) (k+r+\alpha) z^{k+r} \\
&\quad - \sum_{k=0}^{+\infty} c_k \left[ \beta (k+r) + \frac{1}{2} (\delta + \beta + \alpha\beta) \right] z^{k+r+1} \\
&\quad - \sum_{k=0}^{+\infty} c_k [2(k+r) - \gamma + \alpha + 2] z^{k+r+2}.
\end{aligned}$$

We redefine the summation index  $k$  to  $k = m + 2$ ,  $k = m + 1$ , and  $k = m$  for the upper, middle, and lower rows in the equation above. By doing so, we obtain that

$$\begin{aligned}
0 &= \sum_{m=-2}^{+\infty} c_{m+2} (m+r+2) (m+r+2+\alpha) z^{m+r+2} \\
&\quad - \sum_{m=-1}^{+\infty} c_{m+1} \left[ \beta (m+r+1) + \frac{1}{2} (\delta + \beta + \alpha\beta) \right] z^{m+r+2} \quad (\text{B.6}) \\
&\quad - \sum_{m=0}^{+\infty} c_m [2(m+r+1) - \gamma + \alpha] z^{m+r+2}.
\end{aligned}$$

Demanding that every power of  $z$  is zero in eq. (B.6), we conclude that:

$$c_0 r (r + \alpha) = 0, \quad (\text{B.7a})$$

$$(r+1)(r+1+\alpha)c_1 = \frac{1}{2} [\beta(2r+1+\alpha) + \delta] c_0, \quad (\text{B.7b})$$

while the general term is

$$c_{m+2} M_2 = c_{m+1} M_1 + c_m M_0, \quad m \geq 0, \quad (\text{B.7c})$$

with the coefficients  $M_i$ ,  $i = 0, 1, 2$  being given by

$$M_0 = 2(m+r+1) - \gamma + \alpha, \quad (\text{B.7d})$$

$$M_1 = (m+r+1)\beta + \frac{\delta}{2} + \frac{\beta}{2}(1+\alpha), \quad (\text{B.7e})$$

$$M_2 = (m+r+2)(m+r+2+\alpha). \quad (\text{B.7f})$$

The first condition we must impose on the solution so that it becomes a  $N$ -th degree polynomial, where  $N \in \mathbb{Z}^+$ , is:

$$\gamma - \alpha = 2N + 2. \quad (\text{B.8})$$

## References

- [1] A. G. Riess, et al., Observational evidence from supernovae for an accelerating universe and a cosmological constant, *Astron. J.* 116 (1998) 1009–1038. [arXiv:astro-ph/9805201](#), [doi:10.1086/300499](#).
- [2] S. Perlmutter, et al., Measurements of  $\Omega$  and  $\Lambda$  from 42 High Redshift Supernovae, *Astrophys. J.* 517 (1999) 565–586. [arXiv:astro-ph/9812133](#), [doi:10.1086/307221](#).
- [3] L. Amendola, S. Tsujikawa, *Dark Energy: Theory and Observations*, Cambridge University Press, 2010.
- [4] P. J. Steinhardt, A quintessential introduction to dark energy, *Philosophical Transactions of the Royal Society of London. Series A: Mathematical, Physical and Engineering Sciences* 361 (1812) (2003) 2497–2513. [doi:10.1098/rsta.2003.1290](#).
- [5] E. J. COPELAND, M. SAMI, S. TSUJIKAWA, Dynamics of dark energy, *International Journal of Modern Physics D* 15 (11) (2006) 1753–1935. [doi:10.1142/s021827180600942x](#).
- [6] R. R. Caldwell, R. Dave, P. J. Steinhardt, Cosmological imprint of an energy component with general equation of state, *Physical Review Letters* 80 (8) (1998) 1582–1585. [doi:10.1103/physrevlett.80.1582](#).
- [7] V. V. Kiselev, Quintessence and black holes, *Classical and Quantum Gravity* 20 (6) (2003) 1187–1197. [doi:10.1088/0264-9381/20/6/310](#).
- [8] P. S. Letelier, Clouds of strings in general relativity, *Physical Review D* 20 (6) (1979) 1294–1302. [doi:10.1103/physrevd.20.1294](#).
- [9] B. Toshmatov, Z. Stuchlík, B. Ahmedov, Rotating black hole solutions with quintessential energy, *The European Physical Journal Plus* 132 (2) (Feb. 2017). [doi:10.1140/epjp/i2017-11373-4](#).
- [10] S. Chaudhary, M. D. Sultan, A. Malik, A. ur Rehman, A. Övgün, A. A. Ghfar, Images and stability of black hole with cloud of strings and quintessence in egup framework, *Nuclear Physics B* 1006 (2024) 116635. [doi:10.1016/j.nuclphysb.2024.116635](#).

- [11] A. Kumar, S. G. Ghosh, A. Wang, Effect of dark energy on photon orbits and thermodynamic phase transition for hayward anti-de sitter black holes, *Physics of the Dark Universe* 46 (2024) 101608. doi:[10.1016/j.dark.2024.101608](https://doi.org/10.1016/j.dark.2024.101608).
- [12] J. Rayimbaev, U. Eshimbetov, B. Majeed, A. Abdujabbarov, A. Abduvokhidov, B. Abdulazizov, A. Xalmirzayev, Test particles and quasiperiodic oscillations around kiselev black hole with cloud of strings\*, *Chinese Physics C* 48 (5) (2024) 055104. doi:[10.1088/1674-1137/ad2060](https://doi.org/10.1088/1674-1137/ad2060).
- [13] R. Saadati, F. Shojai, Thin shell collapse in kiselev geometry, *Classical and Quantum Gravity* 38 (13) (2021) 135025. doi:[10.1088/1361-6382/abfed5](https://doi.org/10.1088/1361-6382/abfed5).
- [14] R. Wang, F. Gao, H. Chen, Particle dynamics around a static spherically symmetric black hole in the presence of quintessence, *Physics of the Dark Universe* 40 (2023) 101189. doi:[10.1016/j.dark.2023.101189](https://doi.org/10.1016/j.dark.2023.101189).
- [15] M. Malligawad, S. Narasimhamurthy, Z. Nekouee, B. Yashwanth, Shadow analysis and light deflection in charged finslerian kiselev black holes under spherical accretion, *Annals of Physics* 477 (2025) 170005. doi:[10.1016/j.aop.2025.170005](https://doi.org/10.1016/j.aop.2025.170005).
- [16] A. Al-Badawi, F. Ahmed, A new black hole coupled with nonlinear electrodynamics surrounded by quintessence: Thermodynamics, geodesics, and regge–wheeler potential, *Chinese Journal of Physics* 94 (2025) 185–203. doi:[10.1016/j.cjph.2025.01.021](https://doi.org/10.1016/j.cjph.2025.01.021).
- [17] A. Sood, A. Kumar, J. K. Singh, S. G. Ghosh, Photon orbits and phase transitions in kiselev-ads black holes from  $f(r, t)$  gravity, *The European Physical Journal C* 84 (8) (Aug. 2024). doi:[10.1140/epjc/s10052-024-13251-1](https://doi.org/10.1140/epjc/s10052-024-13251-1).
- [18] V. Lungu, M.-A. Dariescu, C. Stelea, Charged particles orbiting a magnetized black hole immersed in quintessential matter, *Physical Review D* 111 (6) (2025) 064014. doi:[10.1103/physrevd.111.064014](https://doi.org/10.1103/physrevd.111.064014).
- [19] F. Javed, M. H. Alshehri, Impact of charged and quantum-correction on the dynamics of scalar shell surrounded by kiselev black hole, *Annals of Physics* 464 (2024) 169658. doi:[10.1016/j.aop.2024.169658](https://doi.org/10.1016/j.aop.2024.169658).

- [20] M.-A. Dariescu, C. Dariescu, Dirac fermions around schwarzschild black holes with quintessence, *General Relativity and Gravitation* 56 (2) (Jan. 2024). [doi:10.1007/s10714-024-03202-2](https://doi.org/10.1007/s10714-024-03202-2).
- [21] DESI Collaboration, DESI 2024 III: Baryon Acoustic Oscillations from Galaxies and Quasars, arXiv e-prints (2024) [arXiv:2404.03000](https://arxiv.org/abs/2404.03000)[arXiv:2404.03000](https://arxiv.org/abs/2404.03000), [doi:10.48550/arXiv.2404.03000](https://doi.org/10.48550/arXiv.2404.03000).
- [22] DESI Collaboration, DESI 2024 IV: Baryon Acoustic Oscillations from the Lyman Alpha Forest, arXiv e-prints (2024) [arXiv:2404.03001](https://arxiv.org/abs/2404.03001)[arXiv:2404.03001](https://arxiv.org/abs/2404.03001), [doi:10.48550/arXiv.2404.03001](https://doi.org/10.48550/arXiv.2404.03001).
- [23] DESI Collaboration, DESI 2024 VI: Cosmological Constraints from the Measurements of Baryon Acoustic Oscillations, arXiv e-prints (2024) [arXiv:2404.03002](https://arxiv.org/abs/2404.03002)[arXiv:2404.03002](https://arxiv.org/abs/2404.03002), [doi:10.48550/arXiv.2404.03002](https://doi.org/10.48550/arXiv.2404.03002).
- [24] DESI Collaboration, DESI DR2 Results II: Measurements of Baryon Acoustic Oscillations and Cosmological Constraints, arXiv e-prints (Mar. 2025). [arXiv:2503.14738](https://arxiv.org/abs/2503.14738), [doi:10.48550/ARXIV.2503.14738](https://doi.org/10.48550/ARXIV.2503.14738).
- [25] L. A. Escamilla, W. Giarè, E. Di Valentino, R. C. Nunes, S. Vagnozzi, The state of the dark energy equation of state circa 2023, *JCAP* 2405 (2024) 091 2024 (05) (2023) 091. [arXiv:2307.14802](https://arxiv.org/abs/2307.14802), [doi:10.1088/1475-7516/2024/05/091](https://doi.org/10.1088/1475-7516/2024/05/091).
- [26] S. Vagnozzi, R. Roy, Y.-D. Tsai, L. Visinelli, M. Afrin, A. Allahyari, P. Bambhaniya, D. Dey, S. G. Ghosh, P. S. Joshi, K. Jusufi, M. Khodadi, R. K. Walia, A. Övgün, C. Bambi, Horizon-scale tests of gravity theories and fundamental physics from the event horizon telescope image of sagittarius A \*, *Classical and Quantum Gravity* 40 (16) (2023) 165007. [doi:10.1088/1361-6382/acd97b](https://doi.org/10.1088/1361-6382/acd97b).
- [27] F. Ahmed, The generalized klein–gordon oscillator in the background of cosmic string space-time with a linear potential in the kaluza–klein theory, *The European Physical Journal C* 80 (3) (Mar. 2020). [doi:10.1140/epjc/s10052-020-7781-5](https://doi.org/10.1140/epjc/s10052-020-7781-5).
- [28] E. Elizalde, Series solutions for the klein-gordon equation in schwarzschild space-time, *Physical review D: Particles and fields* 36 (1987) 1269–1272. [doi:10.1103/PhysRevD.36.1269](https://doi.org/10.1103/PhysRevD.36.1269).

- [29] E. O. Pinho, C. C. Barros, Spin-0 bosons near rotating stars, *The European Physical Journal C* 83 (8) (Aug. 2023). [doi:10.1140/epjc/s10052-023-11907-y](https://doi.org/10.1140/epjc/s10052-023-11907-y).
- [30] L. C. N. Santos, C. C. Barros, Relativistic quantum motion of spin-0 particles under the influence of noninertial effects in the cosmic string spacetime, *The European Physical Journal C* 78 (1) (Jan. 2018). [doi:10.1140/epjc/s10052-017-5476-3](https://doi.org/10.1140/epjc/s10052-017-5476-3).
- [31] L. C. N. Santos, C. C. Barros, Scalar bosons under the influence of non-inertial effects in the cosmic string spacetime, *The European Physical Journal C* 77 (3) (Mar. 2017). [doi:10.1140/epjc/s10052-017-4732-x](https://doi.org/10.1140/epjc/s10052-017-4732-x).
- [32] L. C. N. Santos, C. E. Mota, C. C. Barros Jr., Klein–Gordon Oscillator in a Topologically Nontrivial Space-Time, *Adv. High Energy Phys.* 2019 (2019) 2729352. [doi:10.1155/2019/2729352](https://doi.org/10.1155/2019/2729352).
- [33] A. R. Soares, R. L. L. Vitória, H. Aounallah, On the Klein–Gordon oscillator in topologically charged Ellis–Bronnikov-type wormhole spacetime, *Eur. Phys. J. Plus* 136 (9) (2021) 966. [doi:10.1140/epjp/s13360-021-01965-0](https://doi.org/10.1140/epjp/s13360-021-01965-0).
- [34] R. L. L. Vitória, K. Bakke, On the interaction of the scalar field with a Coulomb-type potential in a spacetime with a screw dislocation and the Aharonov-Bohm effect for bound states, *Eur. Phys. J. Plus* 133 (11) (2018) 490. [doi:10.1140/epjp/i2018-12310-9](https://doi.org/10.1140/epjp/i2018-12310-9).
- [35] R. L. L. Vitória, K. Bakke, Rotating effects on the scalar field in the cosmic string spacetime, in the spacetime with space-like dislocation and in the spacetime with a spiral dislocation, *Eur. Phys. J. C* 78 (3) (2018) 175. [doi:10.1140/epjc/s10052-018-5658-7](https://doi.org/10.1140/epjc/s10052-018-5658-7).
- [36] M. Deglmann, L. Barbosa, C. Barros, Black strings and string clouds embedded in anisotropic quintessence: Solutions for scalar particles and implications, *Annals of Physics* 475 (2025) 169948. [doi:10.1016/j.aop.2025.169948](https://doi.org/10.1016/j.aop.2025.169948).
- [37] J. P. Lemos, Three dimensional black holes and cylindrical general relativity, *Physics Letters B* 353 (1) (1995) 46–51. [doi:10.1016/0370-2693\(95\)00533-q](https://doi.org/10.1016/0370-2693(95)00533-q).

- [38] J. P. S. Lemos, V. T. Zanchin, Rotating charged black strings and three-dimensional black holes, *Physical Review D* 54 (6) (1996) 3840–3853. [doi:10.1103/physrevd.54.3840](https://doi.org/10.1103/physrevd.54.3840).
- [39] M. S. Ali, F. Ahmed, S. G. Ghosh, Black string surrounded by a static anisotropic quintessence fluid, *Annals of Physics* 412 (2020) 168024. [doi:10.1016/j.aop.2019.168024](https://doi.org/10.1016/j.aop.2019.168024).
- [40] A. Ronveaux, F. M. Arscott, Heun’s differential equations, Clarendon Press, 1995.
- [41] D. Batic, R. Williams, M. Nowakowski, [Potentials of the heun class](#), *Journal of Physics A: Mathematical and Theoretical* 46 (2013) 245204. [doi:10.1088/1751-8113/46/24/245204](https://doi.org/10.1088/1751-8113/46/24/245204).  
URL <https://iopscience.iop.org/article/10.1088/1751-8113/46/24/245204>
- [42] B. D. B. Figueiredo, [Schrödinger equation as a confluent heun equation](#), *Physica Scripta* 99 (2024) 055211. [doi:10.1088/1402-4896/ad3510](https://doi.org/10.1088/1402-4896/ad3510).  
URL <https://iopscience.iop.org/article/10.1088/1402-4896/ad3510>
- [43] M. Hortaçsu, Heun functions and some of their applications in physics, *Advances in High Energy Physics* 2018 (2018) 1–14. [doi:10.1155/2018/8621573](https://doi.org/10.1155/2018/8621573).
- [44] D. Petroff, [Slowly rotating homogeneous stars and the heun equation](#), *Classical and Quantum Gravity* 24 (2007) 1055–1068. [doi:10.1088/0264-9381/24/5/003](https://doi.org/10.1088/0264-9381/24/5/003).  
URL <https://iopscience.iop.org/article/10.1088/0264-9381/24/5/003>
- [45] A. G. M. Schmidt, M. E. Pereira, An application of heun functions in the quantum mechanics of a constrained particle, *Journal of Mathematical Physics* 64 (4) (Apr. 2023). [doi:10.1063/5.0135385](https://doi.org/10.1063/5.0135385).
- [46] H. Vieira, V. Bezerra, Confluent heun functions and the physics of black holes: Resonant frequencies, hawking radiation and scattering of scalar waves, *Annals of Physics* 373 (2016) 28–42. [doi:10.1016/j.aop.2016.06.016](https://doi.org/10.1016/j.aop.2016.06.016).

- [47] F. Ahmed, A. Al-Badawi, I. Sakalli, Cylindrically symmetric ads black string surrounded by a cloud of strings and quintessence: geodesics motions, scalar perturbations and thermodynamics (2025). [doi:10.2139/ssrn.5134035](https://doi.org/10.2139/ssrn.5134035).
- [48] Planck Collaboration, Planck 2013 results. xvi. cosmological parameters, *Astronomy and Astrophysics* 571 (2014) A16. [doi:10.1051/0004-6361/201321591](https://doi.org/10.1051/0004-6361/201321591).
- [49] E. Butkov, *Mathematical Physics*, A-W series in advanced physics, Addison-Wesley Publishing Company, 1968.  
URL [https://books.google.com.br/books?id=aGwN1A\\_i3pkC](https://books.google.com.br/books?id=aGwN1A_i3pkC)
- [50] M. Abramowitz, I. A. Stegun, Handbook of mathematical functions with formulas, graphs, and mathematical tables, Vol. 55, US Government printing office, 1968.
- [51] F. Olver, N. I. of Standards, T. (U.S.), *NIST Handbook of Mathematical Functions Hardback and CD-ROM*, Cambridge University Press, 2010.  
URL <https://books.google.com.br/books?id=3I15Ph1Qf38C>